# CHARACTERIZATION OF THE BINDING ACTIVITY OF IMMOBILIZED DNA APTAMERS FOR NUCLEOTIDE AND NON-NUCLEOTIDE TARGETS

A Thesis
Presented to
The Academic Faculty

by

Adam Dunaway

In Partial Fulfillment
of the Requirements for the Degree
Masters of Science in
Bioengineering

Georgia Institute of Technology
December 2014

# CHARACTERIZATION OF THE BINDING ACTIVITY OF IMMOBILIZED DNA APTAMERS FOR NUCLEOTIDE AND NON-NUCLEOTIDE TARGETS.

Approved by:

Dr. Valeria Milam, Advisor
School of Materials Science and Engineering
*Georgia Institute of Technology*

Dr. Johnna Temenoff
School of Biomedical Engineering
*Georgia Institute of Technology*

Dr. Dong Qin
School of Materials Science and Engineering
*Georgia Institute of Technology*

Date Approved: 11-20-14

# ACKNOWLEDGEMENTS

I would like to thank all those who were there with me throughout this process. Dr. Milam without your guidance and dedication as a teacher and adviser this project could have never been accomplished. Thank you for your help through all the highs and lows of my time at Tech. Rich Sullivan, your particular brand of humor, genius, and madness were irreplaceable and helped me to bear the long hours of research. I can never thank you enough for your friendship and guidance these last few years. To Mealing Tapp, Didi Eze, Jonathan Davis, Katie Siegel, Natalie Darby, and Alex Weller, thank you for your help, wisdom, and hard work. It was a pleasure working with each of you. I would also like to thank my committee for their time and efforts in the process of completing this thesis.

To Will McAlexander, Michael Wilson, David Caldwell, Alli and Robert Wear, Kyle and Samantha Crabtree, Jeremiah Glass, and Alex Schaffer, each of your friendships mean the world to me. Thank you for sticking with me through thick and thin from undergraduate all the way through grad school.

To Kaity Moriairity, thank you for putting up with me while I was stressed out and under numerous deadlines, and most importantly for allowing me to share my burdens so that they never became unbearable.

To my parents, whose faith in me never ran dry, thank you for raising me to never give up and to value hard work and education. Without the lessons you instilled in my, this thesis could never have been completed.

Finally and most importantly, I owe all of this to Christ, who made me what I am and lead me to this path.

## TABLE OF CONTENTS


Page

ACKNOWLEDGEMENTS iii

LIST OF TABLES vi

LIST OF FIGURES vii

LIST OF SYMBOLS AND ABBREVIATIONS viii

SUMMARY xi

CHAPTER

1 Literature Review 1

1.1 Colloidal Particles: Interactions and Aggregation 2

1.2 - Deoxyribonucleic Acid as a Biological Macromolecule 4

1.3 Vascular Endothelial Growth Factor as a Therapeutic Target 12

1.4 Summary and Impact of Research 14

1.5 REFERENCES 15

2 Optimizing Aptamer Immobilization and Binding of the Primary DNA Target 18

2.1 Experimental Setup 18

2.2 Results and Discussion 24

2.3 Conclusions 32

2.4 REFERENCES 33

3 Optimizing Specific Binding of VEGF Binding to VEGF Aptamer Functionalized Colloidal Particles 33

3.1 Experimental Setup 33

3.2 Results and Discussion 38

3.3 Conclusions 48

3.4 REFERENCES 49

4 Competitive Binding of VEGF and Complementary DNA to Aptamer Funcitonalized Colloidal Particles 50

4.1 Experimental Setup 50

4.2 Results and Discussion 53

4.3 Conclusions 59

4.4 REFERENCES 59

5 Regeneration of Aptamer Functionalized Colloidal Particles Through DNA Mediated Interactions 60

5.1 Experimental Setup 61

5.2 Results and Discussion 62

5.3 Conclusions 65

5.4 Future Outlook 66

5.5 References 66

APPENDIX A: Calculation of the Radius of Gyration and PEG and **VA1** Aptamer Sequence 67

APPENDIX B: Calculation of the DNA Concentration via UV-vis Spectral Analysis 68

# LIST OF TABLES


| | Page |
|---|---|
| Table 2.1.1: DNA Sequences, Name, and Function | 18 |
| Table 3.2.1: Luminex Standards Calibration and Measurement Data | 40 |
| Table A.1: Measurement of DNA Concentration Using Spectral Analysis | 67 |

# LIST OF FIGURES


Page

Figure 1.1.1: DLVO Theory: Potential Energy Curves 3

Figure 1.2.1: Watson-Crick Base Pairing 5

Figure 1.2.2: DNA Duplex Structure 5

Figure 1.2.3: Aptamer Target Binding Theories 8

Figure 1.2.4: General SELEX Process 9

Figure 1.3.1: Ribbon Structure of Vascular Endothelial Growth Factor Homodimer 13

Figure 2.1.1: Predicted Aptamer Self-Folded Secondary Structures 20

Figure 2.1.2: EDAC Coupling Reaction 22

Figure 2.2.1: Primary Hybridization of DNA-Functionalized Microspheres 25

Figure 2.2.2: Effects of Altering Microsphere Concentration on Primary Hybridization 26

Figure 2.2.3: Effects of PEG and **T7** Sequence as a Blocking Agent 28

Figure 2.2.4: Predicted Homodimer Structure of Aptamer and Probe Sequences 29

Figure 2.2.5: Aptamer Mediated Aggregation of Functionalized Microspheres 31

Figure 2.2.6: Effects of Heat Treatment of Primary Hybridization 31

3.1.1: VEGF Labeling Process 36

3.2.1: Analysis of VEGF Remaining in Supernatant Post Incubation with Aptamer-Functionalized Microspheres 39

3.2.2: VEGF Concentration Calibration Curves 40

3.2.3: Negative Controls for VEGF Concentration Measurements 42

3.2.4: Measurements of VEGF Remaining in Supernatant 43

3.2.5: Detection Limit of VEGF vis Flow Cytometry 44

3.2.6: Effects of **T7** Blocking Agent of Nonspecific Binding of VEGF 45

3.2.7: Lifespan of EDAC Activity on Particle Surface 46

3.2.8: Effect of Aging the Aptamer-Functionalized Particles on VEGF Binding 47

3.2.9: Effect of Heat Treatment on VEGF Binding Activity 48

4.1.1: Coincubation and Serial Incubation of Primary Aptamer Targets 51

4.1.2: VEGF Labeling Process 52

4.2.1: Effects of VEGF Presence Prior to, Following, and During Primary Hybridization 54

4.2.2: Noncomplementary Controls for the Effects of VEGF on Primary Hybridization 56

4.2.3: Effects of VEGF Presence on Primary Hybridization of Ampicillin Aptamer-Functionalized Microspheres 57

4.2.4: Effects of the Presence of Primary DNA Target on VEGF Binding of **VA1**-Funcitonalized Microspheres 58

5.1.1: Recovery of Aptamer Primary Target Binding Activity after Displacement of Priamry DNA Target Using a Displacement Agent 61

5.2.1: Assessing the Recovery of DNA Target Binding Activity After Displacement of Primary DNA Target 64

5.2.2: Assessing the Recovery of VEGF Target Binding Activity After Displacement of Primary DNA Target 65

A.1: UV-vis Spectral Analysis of DNA in Solution 68

# LIST OF ABBREVIATIONS

| | |
|---|---|
| DNA | Deoxyribonucleoic Acid |
| RNA | Ribonucleic Acid |
| SELEX | Systematic Evolution of Ligands by Exponential Enrichment |
| VEGF | Vascular Endothelial Growth Factor |
| EDAC | 1-ethyl-3-[3-dimethylaminopropyl]-carbodiimide hydrochloride |
| PBS | Phosphate Buffered Saline |
| PBS/T | Phosphate Buffered Saline Tween |
| PBS/BSA | Phosphate Buffered Saline Containing Bovine Serum Albumin |
| TE | Tris-EDTA |
| FAM | Carboxyfluorescein |
| PE | Phycoerythrin |
| PEG | Polyethylene Glycol |
| HPLC | High Performance Liquid Chromatography |
| MW | Molecular Weight |
| FSC | Forward Scatter |
| SSC | Side Scatter |
| RT | Room Temperature |
| DLVO | Derjaguin, Landau, Verwey, and Overbeek Theory |
| Au NPs | Gold Nanoparticles |
| PCR | Polymerase Chain Reaction |
| dNTP | Deoxynucleotide Triphosphate |
| A | Adenine |
| G | Gaunine |
| C | Cytosine |

| | |
|---|---|
| T | Thymine |
| AMD | Age Related Macular Degeneration |
| PA | Pre-Annealed |
| AD | Annealed During |
| NA | No Anneal |
| SA | Streptavidin |
| MESF | Molecules of Equivalent Soluble Fluorophore |

## LIST OF SYMBOLS

| | |
|---|---|
| $\Delta G$ | Gibbs Free Energy |
| $\Delta H$ | Enthalpy |
| $\Delta S$ | Entropy |
| $T_m$ | Melting Temperature |
| V | Volume |
| A | Absrobance |
| $\varepsilon$ | Extinction Coefficient |
| l | Length |
| c | Concentration |
| $R_g$ | Radius of Gyration |
| R | Radius |
| $C_\infty$ | Flory-Huggins Parameter |
| n | Number |
| $L_p$ | Persistance Length |

# SUMMARY

This thesis expands prior work with DNA aptamers to investigate the nature of target molecule binding and hybridization of a set of preselected aptamers for vascular endothelial growth factor (VEGF). This work is motivated by the need for better understanding of the interplay between hybridization activity and non-nucleotide target molecule binding to aptamers in order to optimize aptamer-functionalized colloidal therapeutics and diagnostic tools using aptamers. Previous work established that it was possible to induce release of bound VEGF from aptamers using primary hybridization of complementary DNA as a release trigger. These studies expand on this concept by utilizing secondary hybridization events to then release the primary DNA target to recycle or regenerate the aptamer for subsequent binding and release events with either VEGF or with DNA targets. This body of work explores methods to maximize primary and secondary hybridization efficiency and aptamer binding while minimizing understandable nonspecific interactions with the aptamer-functionalized colloidal particles. Chapter 1 provides an overview of colloidal particles, DNA and its properties, aptamers, VEGF, and previous applications of aptamers in therapeutic schemes. Chapter 2 discusses the selection of the DNA aptamers and sequences of interest and details the steps taken to optimize primary hybridization of aptamer functionalized microspheres. Chapter 3 focuses on controlling the binding of VEGF to the aptamer functionalized colloidal particles. Chapter 4 analyzes the nature of competitive binding and displacement of both complementary DNA and VEGF. Chapter 5 discusses the applications of secondary hybridization to enable a recyclable colloidal vehicle.

# CHAPTER 1

# LITERATURE REVIEW

## Introduction

The use of deoxyribonucleic aptamers has become more prevalent over the last decade. Aptamers are oligonucleotides with high specificity and affinity to non-nucleotide targets ranging from molecules such as theophyline to macromolecules such as cell proteins.[1] The interest in deoxyribonucleic acid (DNA) aptamers stems from its unique properties as ligands and ability to modify the DNA macromolecule. Specifically the ability to select, synthesize, and immobilize DNA aptamers to material surfaces has the potential to surpass the decades older process of using antibodies, cutting down the time required to identify, design, and implement therapeutics solutions. Additionally, tailoring the complementarity, melting temperature, and length of the DNA sequences allows for controlled interactions between the aptamer ligand, its non-nucleotide target molecule, and one or more nucleotide target (e.g. DNA, RNA) to design delivery vehicles with programmable release of therapeutics as well as recyclable or regenerative binding capabilities. Polymer microspheres have been used as a substrate for immobilized DNA for the purpose of serving as a model therapeutic delivery vehicle.[2-4]This literature review will outline the fundamentals of colloidal interactions of these polymer microparticles as well as, the role of DNA as a biological macromolecule, aptamer-non-nucleotide target interactions and aptamer selection, and highlight the relevance of vascular endothelial growth factor (VEGF) as a target for clinical use.

## 1.1 Colloidal Particles: Interactions and Aggregation

### *1.1.1 - Colloidal Particles and Size Regimes*

At the colloidal size regime surface-based interactions dominate in determining the behavior of the colloidal systems, meaning that factors such as the presence of charged functional groups, adsorbed molecules, and solution conditions such as pH, ionic strength, and temperature play a significant role in determining the behavior of suspensions.[5] Typically, particles possessing a single dimension between $10^{-3}$ and 1 μm fit this description, but some particle dimensions can exist outside of this range.[6-8] Various shapes and compositions are available in colloidal species, but surface composition often dominates in determining the observed behavior in a colloidal suspension. As a result colloidal suspensions can display a wide variety of phase behavior ranging from fluid like systems of repulsive particles at a dilute concentration to more highly concentrated gels formed from attractive particles.[9] Fluorescence microscopy, confocal microscopy, flow cytometry, and spectroscopy are some of the multitude of tools available for the characterization of colloidal suspensions, allowing researchers to analyze the structure within the suspensions or investigate surface functionalities found on the particle surfaces.[10] Nonspecific interactions such as repulsive electrostatic, attractive van der Waals, and repulsive steric interactions are commonly used to control colloidal interactions and the resulting phase behavior.[9] The classic Derjaguin, Landau, Verwey, and Overbeek (DLVO) theory is commonly used to predict colloidal stability of homogeneous suspensions in polar mediums and accounts for electrostatic and van der Waals interactions.[11] Figure 1.1.1 is a representative schematic of DVLO interaction potential energy curves and their effect on particle interactions.

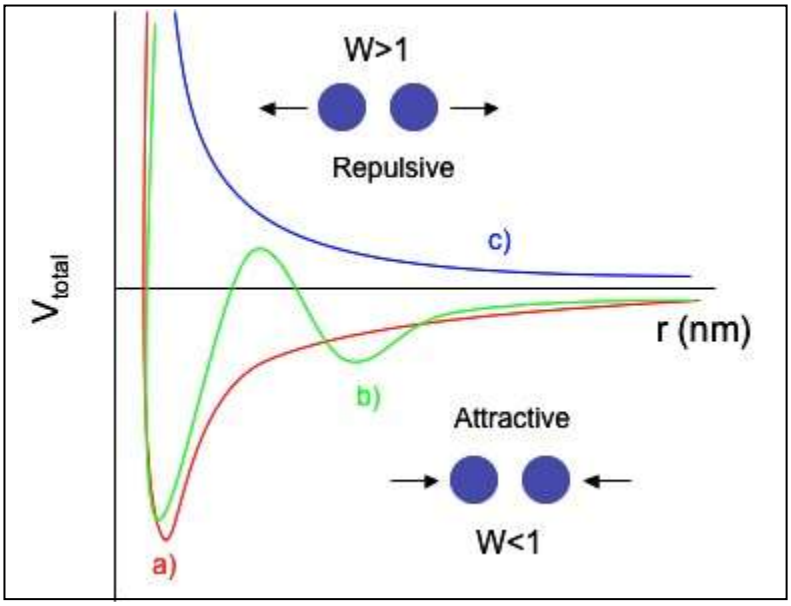


**Figure 1.1.1:** Schematic representation of the distant-dependent DLVO potential energy curves for a pair of identical particles. a) A deep primary attractive well that results in irreversibly aggregated particles, b) a secondary attractive well, causing weaker reversible attraction between particles at a larger separation distance, and c) a completely repulsive interaction potential, yielding stable disperse particles. W is a stability ratio which favors aggregation when less than 1.[5]

While stable suspensions of repulsive identical particles, such a repulsion based approach is typically insufficient to direct the arrangement of neighboring particles, particularly in heterogeneous suspensions comprised of different repulsive particles. To further augment the degree of control over the phase behavior, colloidal surfaces can be functionalized with desirable biomacromolecules capable of mediating specific interactions. In addition to the specific attractive interactions, it should be noted that the polymeric nature of these biomacromolecules can also be used to further stabilize colloidal suspensions through the introduction of entropic effects to steric repulsion interactions. The repulsion creates a system unfavorable to nonspecific aggregation by overcoming attractive van der Waals interactions across small distances. Furthermore, these surface-bound biomacromolecules typically possess charge groups. Thus, while these electrostatic effects can mask nonspecific attractive interactions, one typically must add sufficient counter ion species in order to allow for match biomacromolecules such as DNA to bind to one another across opposing particle surfaces. Classic examples of

employing specific interactions to mediate colloidal interactions can be found in the early work of Mirkin et al.[16] and Alivisatos et al.[17] have previous published reports on DNA-based nanoparticle assembly. Their work utilized gold nanoparticles (Au NPs) and immobilized thiolated DNA to bridge surfaces together using DNA hybridization events, allowing them to design complex colloidal aggregates. In separate work by Pena's group, enzymatic extension of the immobilized DNA template[18] and the incorporation of complementary spacer DNA strands has allowed for the incorporation of long DNA strands on particles and brought new levels of diversity to the design of colloidal vehicles.

## 1.2 - Deoxyribonucleic Acid as a Biological Macromolecule

### *1.2.1 - Deoxyribonucleic Acid and its Properties*

Oligonucleotides are biological polymers composed from repeating nucleotide units.[19] Nucleotides consist of alternating five carbon deoxyribose sugar group and negatively charged phosphate to form the deoxyribonucleic backbone. Additionally, one of four following nitrogenous bases are attached as a side group: adenine (A), guanine (G), cytosine (C), or thymine (T). These bases interact with one another through hydrogen bond formation during the formation of a deoxyribonucleic acid (DNA) duplex. Below a schematic of the four bases and the specific Watson-Crick base interactions between purines (G, A) and pyrimidines (C, T) is shown in Figure 1.2.1 in which adenine specifically binds only to thymine, and cytosine binds only to guanine.

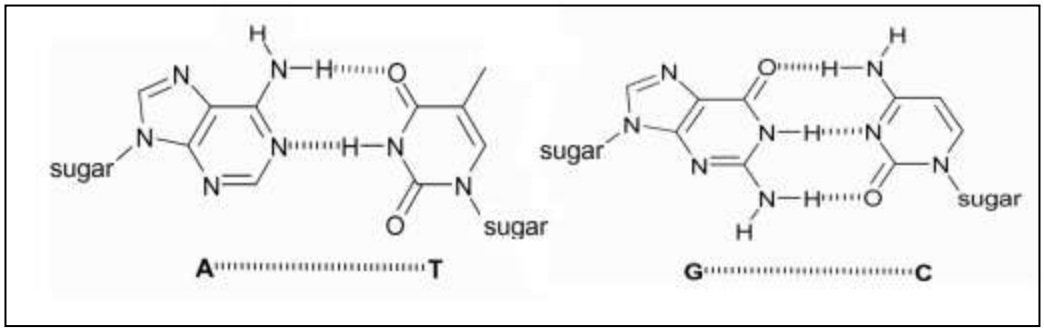


**Figure 1.2.1:** Hydrogen bonding according to Watson-Crick base pair interactions, showing the characteristic three hydrogen bonds between guanine (G) and cytosine (C) and two hydrogen bonds between adenine (A) and thymine (T). Taken from Gothelf and LaBeen.[20]

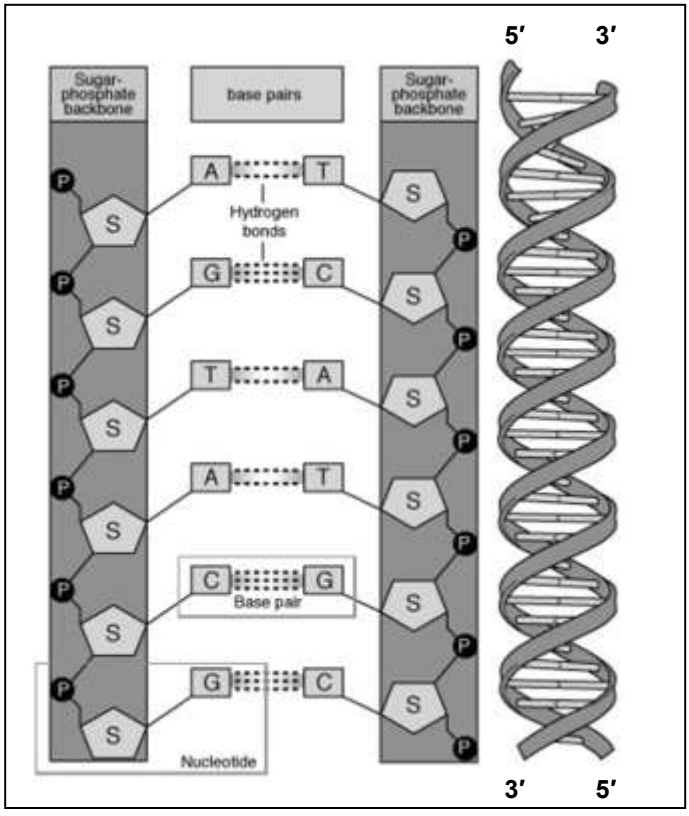


**Figure 1.2.2:** Schematic illustration of DNA duplex comprised of two complementary sequences that hybridize to form an anti-parallel helix in which the central core is comprised of hydrophobic bases while the periphery of the duplex is comprised of the hydrophilic sugar-phosphate backbone. Adapted from http://www.accessexcellence.org/RC/VL/GG/dna2.php, accessed 11/7/2104)

As illustrated in Figure 1.2.2, the classical double helical structure of DNA is then formed from two anti-parallel nucleotide chains held together by the base interactions and

stacking contributions from the pi bonds found with the bases. This regular structure and the redundancy of the complementary strands makes DNA an excellent choice for the storage of genetic information. Compared to RNA, the deoxygenated sugar group of DNA offers greater resistance to nuclease degradation *in vivo*, and it has base specificity that serves as a critical factor in DNA replication and the transcription of DNA to RNA for protein synthesis allowing for high fidelity throughout generations of cells.

### 1.2.2 Biological Function of DNA

DNA is a central molecule in the function of all cellular processes. It serves as a coding source for the genetic material of all organisms and acts as a director of the systems in charge of replication, transcription of RNA and ultimately protein synthesis, and silencing of cellular functions.[21] DNA is tightly packed in the nucleus of eukaryotic cells in nucleosomes, long sequences of methylated DNA wrapped around histones. Specific base pairing between the four nucleotides according to Watson-Crick base pairing serves as the basis of the genetic code, ensuring consistency in the genome during protein synthesis and cellular proliferation. With every three nucleotides coding for a different amino acid during transcription, DNA is responsible for the formation of all the proteins within an organism with alternative slicing pathways to ensure that the limited diversity of the four base DNA alphabet allows for the generation of diverse proteins.

### 1.2.3 DNA Aptamer structure, function, selection, and clinical relevance

Aptamers, for the purposes of this thesis, are defined as oligonucleotides capable of specifically binding to a non-oligonucleotide target molecule. These can range from small molecule targets like ampicillin[22] to whole proteins in the case of growth factors.

[23] Aptamers can be derived from ribonucleic acid (RNA) or peptides as well, but DNA aptamers have been gaining notoriety due to the increased nuclease resistance they offer over more traditional RNA systems. Additional attributes include the ease with which they can be altered before and after synthesis to further optimize binding affinity or attach functional groups for various applications. They are also being explored as alternates to more commonly used multivalent ligands such as antibodies for similar reasons. While antibodies have to be extracted from animal fluids following antigen injection, DNA aptamers can be handled and derived inside a test tube through processes involving sequences that are a few dozen to a few hundred nucleotides in length.[24] Aptamers have the potential to fill a similar role as antibodies in clinical use by serving as a targeting agent to relevant biological markers (e.g. cell receptros) *in vivo* or as diagnostic tools capable of verifying the presence of known pathogens or markers associated with specific diseases.[25]

With the increase in interest in oligonucleotides as bio-inspired ligand alternatives to antibodies, it has become important to understand the role of aptamer structure in specific aptamer-target binding interactions. At the time of writing, a number of key questions remain unanswered, but it is important to mention the ongoing uncertainty in the literature regarding the role of primary and secondary aptamer structure in recognition-based binding events. As single stranded oligonucleotides, aptamers are prone to forming secondary structures such as those found in single-stranded RNA (ssRNA) sequences such as the classic stem and loop structure, but is this secondary form necessary to facilitate specific binding, the lock-and-key model,[12, 22] or do base interactions play the dominate role, leading to an induced fit[26] of the aptamer's secondary structure in the presence of the non-nucleotide target as illustrated in Figure 1.2.3. The answer is not as clear as most would like, but select studies have begun to draw links between the role structure and base interactions.[27-29] Currently, the interactions are explained for each aptamer sequence in question, attributing the

specificity to interplay between stacking effects, shape complementarities, electrostatic interactions, or the formation of pseudo-base interactions using hydrogen bonds.[24] Aptamer affinity for a non-nucleotide target is quantified by measuring the equilibrium dissociation constant of the aptamer-target complex.[23] A key focus and challenge of current aptamer research is the development of assays to accurately evaluate the affinity values for a give aptamer-target system

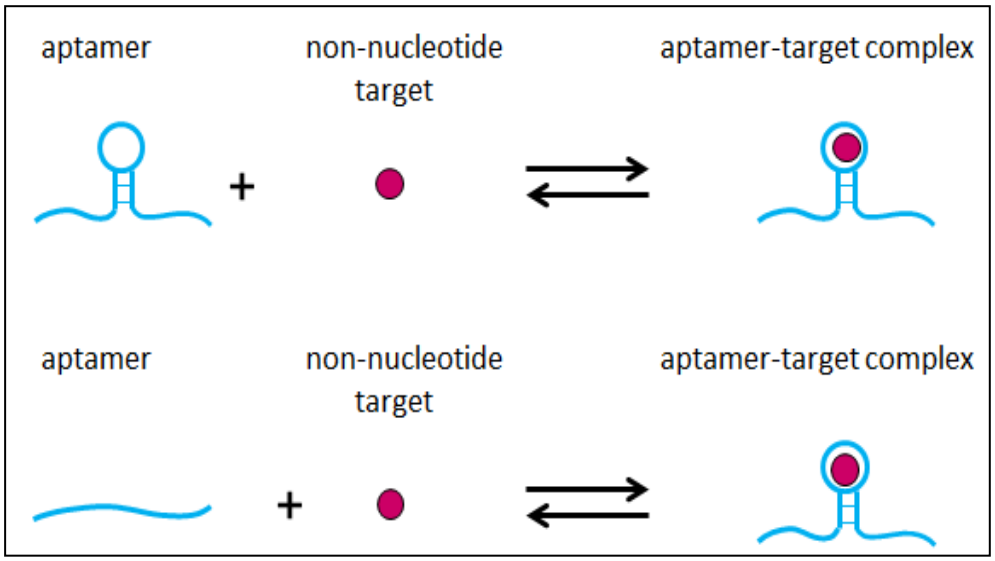


**Figure 1.2.3.** Schematic illustration of (top) lock-and-key and (bottom) induced fit binding between an oligonucleotide aptamer and its non-nucleotide target.

The identification of new oligonucleotide aptamers historically occurs through an *in vitro* process known as the systematic evolution of ligands by exponential enrichment (SELEX).[30] SELEX is a combinational chemistry technique that may be optimized in various ways to allow for the selection of aptamers of greatly varying lengths and targets. Figure 1.2.4 shows a general schematic for the SELEX process.

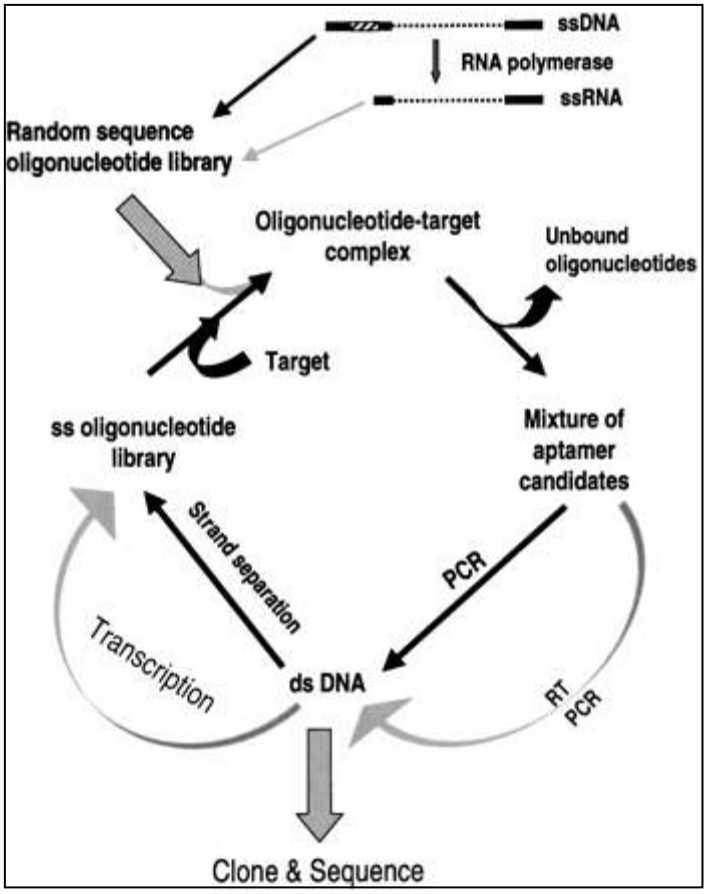


**Figure 1.2.4:** A generalized schematic showing the key steps in a standard SELEX process.[30]The process begins with the generation of a random oligonucleotide library. The library is then incubated with the non-nucleotide target. Following incubation, any unbound oligonucleotides are removed and the bound aptamer candidates are eluted from the target. The recovered oligonucleotides are amplified using polymerase chain reaction (PCR), and the process is repeated for a chosen number of additional rounds, typically 10-20. The final selected aptamer candidates are then recovered and sequenced to reveal their sequence identity.

SELEX is a cyclical process being with the generation of a large pool of random DNA sequences of an arbitrary size. The central randomized segment is flanked by constant primer binding regions at the 5' and 3' ends. Within a segment of base length, n, there exist $4^n$ possible sequences within the random library. This sequence diversity allows researchers to explore a number of candidate aptamer sequence; however the likelihood of exploring all possible sequences within a given SELEX experiment is unlikely as the length, n, is increased.[31] Following the generation of the library, the sequences are then incubated with the target of interest. Following incubation, unbound

oligonucleotides are removed, often by affinity chromatography or a similar process. Elution of the bound sequences is then followed by polymerase chain reaction (PCR) to exponentially amplify the bound aptamer candidates, doubling the amount of product for every cycle of PCR performed. This process can continue until the precursors, DNA primers and deoxynucleotide triphosphates (dNTPs) are exhausted. Subsequent rounds of the selection process are then performed and the stringency of the elution process is altered to narrow down the number of potential candidates to identify the highest affinity aptamer sequences. Aptamer candidates may then be analyzed and sequenced following the final round of SELEX. Additionally, counterSELEX cycles may be included to ensure that the aptamer specifically binds the target substrate rather than a material on which targets are immobilized to or molecules that are chemically or structurally similar to the desired non-nucleotide target. Modifications may also be made post-SELEX to adjust the affinity between an aptamer and target molecule using base deletions, mutations, or extensions.[1, 24, 30]

### 1.2.4 Thermodynamics of DNA in Solution

Duplex melting temperature are important to the understanding of the formation of DNA duplexes through hybridization of two complementary DNA strands. By convention, the melting temperature is defined as the temperature at which half of the duplexes are dissociated. Thus, the melting temperature serves as a measure of the thermal stability of the duplex and affinity of two strands for one another. Ionic strength of the solution, sequence composition, and strand concentration are all deciding factors in determining the melting point of an oligonucleotide system.[32, 33] Melting temperature values can be tailored, for example, by adjusting the C/G and A/T base ratio. Higher amounts of C/G results in a higher melting temperature due to the three hydrogen bonds

formed between cytosine and guanine in comparison to the two hydrogen bonds formed between adenine and thymine. Ionic strength through salt additions affects the melting point by introducing counter ions for the negatively charged phosphate backbone of DNA. Thus, increasing the ionic strength will elevate the melting temperature by providing shielding and lowering the electrostatic repulsive interactions, as shown in equation 1, between DNA strands. The Gibb's free energy is a key thermodynamic "indicator" that takes into account many of these parameters by considering enthalpic and entropic contributions to the system. Additional considerations that are taken into account in current models include the contributions of base-stacking effects to the enthalpy and entropy.[34]

$$\Delta G=\Delta H-T\Delta S \qquad (1)$$

This thermodynamic analysis can be extended to single stranded DNA (ssDNA) and serves as an indicator of the stability of intrastrand secondary structures such as hairpins and loops. DNA strands hybridize in an anti-parallel fashion, and thus ssDNA of sufficient base length can self-fold or self hybridize. Such interactions are important to consider during the selection of aptamers for this work because (1) the formation of homodimers between a population of particles all functionalized with identical DNA sequences DNA functionalized particles and (2) the formation of self hybridized or secondary intrastrand structures of the aptamer as well as (3) formation of aptamer-DNA duplexes must all be considered and monitored to insure the current experimental system functions correctly. Michael Zuker's UNAFold web-server is a powerful tool for this type of analysis, allowing calculation of all three values at varying temperatures and salt concentrations.[35] This online thermodynamic calculator allows for rapid calculation of

DNA and RNA duplex melting temperatures and self melt temperatures and reports values for thermodynamic contributions to the Gibb's free energy for homodimer formation, self hybridization, and heterodimer hybridization. This online tool also displays any secondary structure that could feasibly be formed by the submitted sequence, and generates melting plots for the DNA system of interest.

## 1.3 Vascular Endothelial Growth Factor as a Therapeutic Target

### 1.3.1 Vascular Endothelial Growth Factor Structure and General Physiological Function

Vascular endothelial growth factor (VEGF) is one of numerous identified angiogenic growth factors.[36] It's homodimer structure is shown in Figure 1.3.1. In its native state VEGF is a heparin-binding homodimer glycoprotein, 45,000 Daltons in size.[37, 38] It exists in a number of isoforms: $VEGF_{165}$ $VEGF_{121}$, $VEGF_{189}$, $VEGF_{206}$ are among the most common with $VEGF_{165}$ being the major isoform.[36] $VEGF_{165}$ is basic in nature compared to the acidic $VEGF_{121}$ isoform. The other two isoforms are more basic and bind heparin more readily. $VEGF_{165}$ and $VEGF_{121}$ are soluble proteins and a readily secreted from cells, though the $VEGF_{165}$ has a significant fraction left bound to the surface of cells.

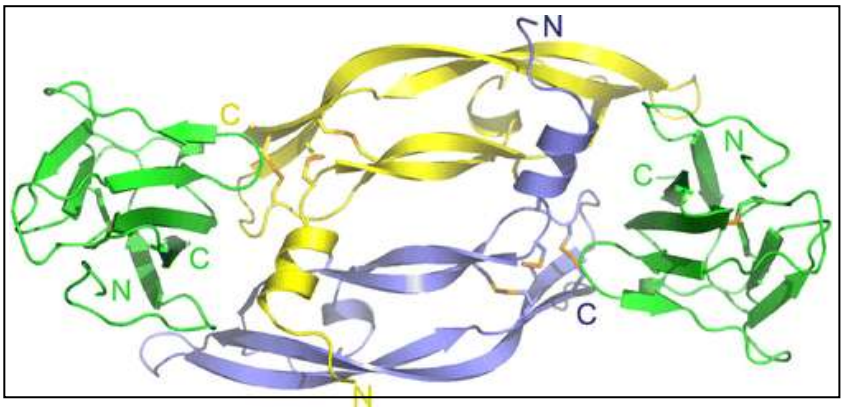


**Figure 1.3.1: Ribbon diagram of two vascular endothelial growth factor (VEGF) molecules (yellow and blue) in their antiparallel homodimer structure attached to two receptor molecules(green). Taken from Ferrara's Vascular Endothelial Growth Factor: Basic Science and Clinical Progress.[39]**

The role of VEGF in angiogenesis and vasculogenesis is to stimulate formation of new blood vessels following injury, during embryonic development, or to bypass blocked vessels[36, 38, 39] by promoting the migration and mitosis of endothelial cells to the injury site and initiating cell proliferation to build the necessary vasculature. Mutations or suppression of the VEGF gene have been linked to embryonic lethality in mice due to underdevelopment of organ vasculature and reduction in red blood cell nucleation. The effects are less pronounced in juvenile primates, leading only to suppression of the growth plate and ovarian angiogenesis.[36] Gradients of VEGF are also linked to directional growth of longitudinal bones and cartilage invasion by blood vessels during skeletal growth and endochondral bone formation.[40]

### 1.3.2 Role of Vascular Endothelial Growth Factor in Diseases

VEGF plays an important role in pathological angiogenesis. VEGF mRNA has been shown to be up regulated in human tumors. Vasculogenesis initiated by the over expressed growth factor allows tumors to grow and metastasize.[39] Diabetes mellitus may result from neovascularization, leading to vitreous hemorrhages, detachment of the retina, and even blindness due to excessive expression of VEGF. It has also been linked to

various inflammatory disorders and infertility in females by contributing to polycystic ovary syndrome.[41]

A number of VEGF inhibitors have been developed to treat malignancy and help moderate gynecologic and ocular diseases. Thus far phase 2 and 3 trials have shown that VEGF inhibition may have a number of optimistic uses in future clinical treatments to minimize pathological angiogenesis, but further tests are needed to optimize such processes. An antibody-based therapeutic called Bevacizumab is the first such inhibitor clinically available in the United States. While other antibodies for growth factors exist or are still in development, Pegaptanib (or Macugen) is an example of an aptamer-based therapeutic that binds to VGEF. This angiogenic medication is used specifically to treat age-related macular degeneration (AMD) by binding the growth factor in the eye and acting as an agent to prevent formation of the vasculature responsible for the disease by reducing associated swelling and minimizing leakage from the blood vessels.[42]

Alternatively, VEGF itself may be desired as a therapeutic agent in cases such as coronary or limb ischemia in which restoration of blood vessel function is desirable. Current clinical treatments have not shown as significant results, but this may be due to under exposure in trials. Vascularization is a time dependent process, requiring more persistent exposure to VEGF to allow the newly forming vasculature to fully develop and prevent regression of the new vessels.[43]

### 1.4 Summary and Impact of Research

This thesis delves into the design and implementation of a colloidal delivery vehicle for the controlled uptake and release of vascular endothelial growth factor (VEGF). Preselected DNA aptamers are immobilized onto the surface of carboxylated microspheres, using 1-ethyl-3-[3-dimethylaminopropyl]-carbodiimide hydrochloride **(**EDAC) to form an amide bond between the aminated aptamer and functional groups. Through use of simple DNA mediated interactions, it is possible to selectively bind and release VEGF.[3, 4, 12] At this point in time, aptamer research is still in its infancy

compared to the decades of devoted research to antibodies and thus the nature of the interaction between an aptamer and its target molecule is still unclear. To elucidate the nature of this interaction in the current work, primary and secondary hybridization of the aptamer sequences is studied and used implemented as a method to regenerate previously bound aptamers the goal of implementing a long term reusable delivery vehicle capable augmenting or even replacing current therapies such as chemotherapy. In order to expand the understanding of aptamer interactions, competitive binding and displacement of both VEGF and complementary soluble DNA sequences from particle-immobilized aptamers are investigated. We believe this work represents an important step forward in elucidating the binding nature of aptamers for their continued use in physiological systems as therapeutic agents. We investigate the effects of heat treatment, primary and secondary hybridization on a series of aptamer binding events to either VEGF or DNA targets.

## 1.5 References


1. Stoltenburg, R., C. Reinemann, and B. Strehlitz, *SELEX-A (r)evolutionary method to generate high-affinity nucleic acid ligands.* Biomolecular Engineering, 2007. **24**(4): p. 381-403.
2. Giljohann, D.A., et al., *Oligonucleotide loading determines cellular uptake of DNA-modified gold nanoparticles.* Nano Letters, 2007. **7**(12): p. 3818-3821.
3. Tison, C.K. and V.T. Milam, *Reversing DNA-Mediated adhesion at a fixed temperature.* Langmuir, 2007. **23**(19): p. 9728-9736.
4. Tison, C.K. and V.T. Milam, *Programming the kinetics and extent of colloidal disassembly using a DNA trigger.* Soft Matter, 2010. **6**(18): p. 4446-4453.
5. Hiemenz, P.C. and R. Rajagopalan, *Principles of Colloid and Surface Chemistry, Third Edition, Revised and Expanded*. 1997: Taylor & Francis.
6. Birdi, K.S., *Surface Chemistry Essentials*. 2013: Taylor & Francis.
7. Russel, W.B., D.A. Saville, and W.R. Schowalter, *Colloidal Dispersions*. 1989: Cambridge University Press.
8. Xia, Y., et al., *Colloids and Colloid Assemblies: Synthesis, Modification, Organization and Utilization of Colloid Particles*. 2006: Wiley.
9. Pusey, P.N. and W. van Megen, *Phase behaviour of concentrated suspensions of nearly hard colloidal spheres.* Nature, 1986. **320**(6060): p. 340-342.
10. Cram, L.S., *Methods in Cell Science.* 2003: p. 1-9.
11. Underwood, S.M., J.R. Taylor, and W. van Megen, *Sterically Stabilized Colloidal Particles as Model Hard Spheres.* Langmuir, 1994. **10**(10): p. 3550-3554.
12. Battig, M.R., B. Soontornworajit, and Y. Wang, *Programmable Release of Multiple Protein Drugs from Aptamer-Functionalized Hydrogels via Nucleic Acid*

*Hybridization.* Journal of the American Chemical Society, 2012. **134**(30): p. 12410-12413.
13. Eze, N.A. and V.T. Milam, *Exploring locked nucleic acids as a bio-inspired materials assembly and disassembly tool.* Soft Matter, 2013. **9**(8): p. 2403-2411.
14. Gold, L. and N. Janjic, *High-affinity oligonucleotide ligands to vascular endothelial growth factor (VEGF).* 1998, Google Patents.
15. Nonaka, Y., K. Sode, and K. Ikebukuro, *Screening and Improvement of an Anti-VEGF DNA Aptamer.* Molecules, 2010. **15**(1): p. 215-225.
16. Mirkin, C.A., et al., *A DNA-based method for rationally assembling nanoparticles into macroscopic materials.* Nature, 1996. **382**(6592): p. 607-609.
17. Xu, X.Y., et al., *Asymmetric functionalization of gold nanoparticles with oligonucleotides.* Journal of the American Chemical Society, 2006. **128**(29): p. 9286-9287.
18. Pena, S.R.N., et al., *Hybridization and enzymatic extension of Au nanoparticle-bound oligonucleotides.* Journal of the American Chemical Society, 2002. **124**(25): p. 7314-7323.
19. Calladine, C.R. and H.R. Drew, *Understanding DNA: the molecule & how it works*. 1992: Academic Press.
20. Gothelf, K.V. and T.H. LaBean, *DNA-programmed assembly of nanostructures.* Organic & Biomolecular Chemistry, 2005. **3**(22): p. 4023-4037.
21. Alberts, B., et al., *Molecular Biology of the Cell, 4th edition.* 2002.
22. Song, K.M., et al., *Aptasensor for ampicillin using gold nanoparticle based dual fluorescence-colorimetric methods.* Analytical and Bioanalytical Chemistry, 2012. **402**(6): p. 2153-2161.
23. Potty, A.S.R., et al., *Biophysical Characterization of DNA Aptamer Interactions with Vascular Endothelial Growth Factor.* Biopolymers, 2009. **91**(2): p. 145-156.
24. Hermann, T. and D.J. Patel, *Biochemistry - Adaptive recognition by nucleic acid aptamers.* Science, 2000. **287**(5454): p. 820-825.
25. Jayasena, S.D., *Aptamers: An emerging class of molecules that rival antibodies in diagnostics.* Clinical Chemistry, 1999. **45**(9): p. 1628-1650.
26. Dittmer, W.U., A. Reuter, and F.C. Simmel, *A DNA-Based Machine That Can Cyclically Bind and Release Thrombin.* Angewandte Chemie International Edition, 2004. **43**(27): p. 3550-3553.
27. Clouetdorval, B., T.K. Stage, and O.C. Uhlenbeck, *Neomycin Inhibition of the Hammerhead Ribozyme Invovles Ionic Interactions.* Biochemistry, 1995. **34**(35): p. 11186-11190.
28. Fan, P., et al., *Molecular recognition in the FMN-RNA aptamer complex.* Journal of Molecular Biology, 1996. **258**(3): p. 480-500.
29. Zimmermann, G.R., et al., *Molecular interactions and metal binding in the theophylline-binding core of an RNA aptamer.* Rna-a Publication of the Rna Society, 2000. **6**(5): p. 659-667.
30. Wilson, D.S. and J.W. Szostak, *In vitro selection of functional nucleic acids.* Annual Review of Biochemistry, 1999. **68**: p. 611-647.
31. Kupakuwana, G.V., et al., *Acyclic Identification of Aptamers for Human alpha-Thrombin Using Over-Represented Libraries and Deep Sequencing.* Plos One, 2011. **6**(5): p. 11.

32. Jin, R.C., et al., *What controls the melting properties of DNA-linked gold nanoparticle assemblies?* Journal of the American Chemical Society, 2003. **125**(6): p. 1643-1654.
33. Park, S.Y. and D. Stroud, *Theory of melting and the optical properties of gold/DNA nanocomposites.* Physical Review B, 2003. **67**(21): p. 4.
34. SantaLucia, J. and D. Hicks, *The thermodynamics of DNA structural motifs.* Annual Review of Biophysics and Biomolecular Structure, 2004. **33**: p. 415-440.
35. Zuker, M., *Mfold web server for nucleic acid folding and hybridization prediction.* Nucleic acids research, 2003. **31**(13): p. 3406-3415.
36. Ferrara, N., H.P. Gerber, and J. LeCouter, *The biology of VEGF and its receptors.* Nature Medicine, 2003. **9**(6): p. 669-676.
37. Ferrara, N. and T. DavisSmyth, *The biology of vascular endothelial growth factor.* Endocrine Reviews, 1997. **18**(1): p. 4-25.
38. Ferrara, N., et al., *Molecular and Biological Properties of the Vascular-Endothelial-Growth-Factor Family of Proteins.* Endocrine Reviews, 1992. **13**(1): p. 18-32.
39. Ferrara, N., *Vascular endothelial growth factor: Basic science and clinical progress.* Endocrine Reviews, 2004. **25**(4): p. 581-611.
40. Sondell, M., G. Lundborg, and M. Kanje, *Vascular endothelial growth factor has neurotrophic activity and stimulates axonal outgrowth, enhancing cell survival and Schwann cell proliferation in the peripheral nervous system.* Journal of Neuroscience, 1999. **19**(14): p. 5731-5740.
41. Yen, S.S.C., *Polycystic Ovary Syndrome.* Clinical Endocrinology, 1980. **12**(2): p. 177-207.
42. Cunningham, E.T., et al., *A phase II randomized double-masked trial of pegaptanib, an anti-vascular endothelial growth factor aptamer, for diabetic macular edema.* Ophthalmology, 2005. **112**(10): p. 1747-1757.
43. Henry, T.D., et al., *Vascular endothelial growth factor in ischemia for vascular angiogenesis.* Circulation, 2003. **107**(10): p. 1359-1365.

# CHAPTER 2

# OPTIMIZING APTAMER IMMOBILIZATION AND BINDING OF THE PRIMARY DNA TARGET

This chapter will detail the initial investigation into the immobilization of aptamer and DNA probe sequences onto microspheres and assess the ability of the immobilized aptamer sequences to bind to their primary DNA target. An EDAC coupling procedure is outlined , and the effects of aptamer concentration and incorporation of a secondary blocking agent are investigated. The focus of these studies was the optimization of binding of the aptamer sequences to DNA to verify hybridization activity of the aptamer and as a first step in designing a colloidal delivery vehicle capable of repeated binding and release events through simple DNA mediated interactions. Thermodynamic data for all of the sequences of interest is included as well as a study investigating the effects of heat treatment of aptamer-functionalized suspensions on hybridization. Ultimately, we uncovered handling parameters to maximize specific hybridization activity of the immobilized aptamers to specific DNA targets.

## 2.1 Experimental Setup

### 2.1.1 Aptamer and Complementary Target Selection

The aptamers used within this work were selected based on reports by Battig *et al.*[1] and Hasegawa *et al.*[2] Table 2.1.1 outlines the sequence information, including the function, name and sequence itself. The nomenclature is as follows: aptamers are named using two letters. The first letter corresponds to the molecule to which it binds: **V** for VEGF and **A** for ampicillin. The second letter is always an **A** to denote that it is an aptamer sequence. Complementary sequences add a **C** to this notation. For instance, **VA1C** corresponds to the primary DNA complementary target for the first VEGF

aptamer sequence, **VA1**. Additionally, a displacement agent (**DA**) sequence is used later, Chapter 5, to displace the primary DNA target. All noncomplementary sequences are denoted as **NC** followed by the number of total bases (e.g. **NC14**. The presence of a FAM label is denoted by ***F** following the sequence name. Finally, a DNA probe and its complementary sequence were used as negative controls for nucleotide (this chapter) and non-nucleotide binding (Chapter 3). They use nomenclature outlined previously in our group.[3] The immobilized probe sequence is denoted with an **A** and its base length. Complementary sequences are denoted with a **B** and the sequence length. Again ***F** following any sequence name indicates FAM- labeling of the 5' end of the DNA.

**Table 2.1.1:** List of function, nomenclature, and sequences. All targets and displacement agents are soluble (i.e. not immobilized on microspheres), and the presence of a FAM dye molecule on the 5' end is indicated with "***F**" in the nomenclature. A toehold region on the 5' ends of the complementary targets is indicated by underlining the sequence and the polythymine spacer (between the particle surface and aptamer sequence segment) is shown as $T_{10}$ within the sequence.

| Function | Name | Sequence |
|---|---|---|
| **VEGF aptamer 1** | **VA1** | **3'-GGGACGTGAGAACAGACCTTCTGCCCT$_{10}$ -5'** |
| **complementary target** | **VA1C**<br>**VA1C*F** | **5'-<u>ACCT</u>CCCTGCACTCTTGTCT -3'** |
| **displacement agent** | **DA** | **3'-<u>TGGA</u>GGGACGTGAGAACAGA-5'** |
| **VEGF aptamer 2** | **VA2** | **3'-TGATAGACCGGGTGTGTGTAGGGCTGTCAT$_{10}$-5'** |
| **complementary target** | **VA2C*F** | **5'–ACTCACTATCTGGCCCACAC – 3'** |
| **ampicillin aptamer** | **AA** | **3'-GGCGATATGTTGGCGGGCGT$_{10}$-5'** |
| **complementary target** | **AAC** | **5'-AAAGGACCGCTATACAAC -3'** |
| **DNA probe** | **A20** | **3'-TAGTCGGCGTTAGGT$_6$-5'** |
| **complementary target** | **B15*F** | **5′-ATCAGCCGCA ATCCA- 3'** |
| **blocking agent** | **T7** | **5'-TTTTTTT-3'** |
| **noncomplementary target** | **NC18*F** | **3'-CAACATATCGCCAGGAAA-5'** |
| **noncomplementary target** | **NC14**<br>**NC14*F** | **3'-GGATTGCGGCTGAT-5'** |

It is important to note that a single-stranded four base long toehold region was incorporated into the primary DNA targets, **VA1C**. The toehold, underlined in Table 1, was shown, using the UNAFold program[4], to not inhibit primary hybridization or form any stable intrastrand secondary structures at room temperature (RT) as shown in Figure 2.1.1. All DNA sequences were synthesized by Integrated DNA Technologies and

purified by the manufacturer using HPLC. 6-carboxyfluorescein (FAM) was used to fluorescently label complementary and noncomplementary sequences. The aminated aptamer and DNA probe sequences were received with the terminal -$NH_2$ group on the 5' end.

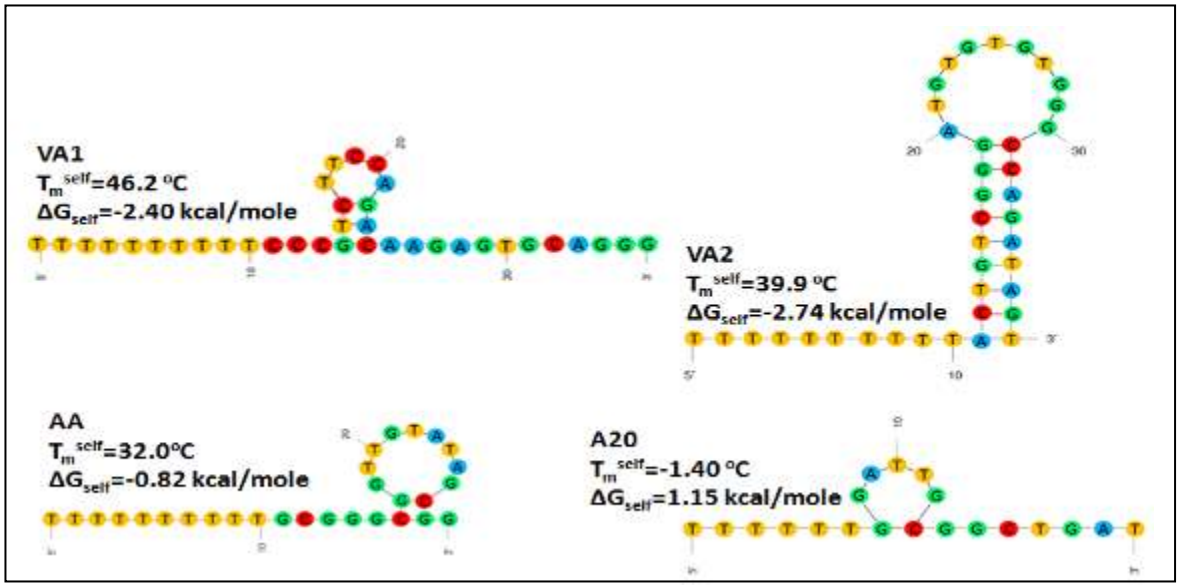


**Figure 2.1.1:** Illustrated drawings adapted from UNAFold based predictions of the most thermodynamically favorable secondary structures for the VEGF Aptamer 1 (**VA1**), VEGF Aptamer 2 (**VA2**), Ampicillin Aptamer (**AA**), and probe (**A20**). The self-melt temperature value, $T_m^{self}$ and intrastrand hybridization Gibbs Free Energy ($\Delta G_{self}$) reported by Zuker's UNAFOLD program[4] are shown for each sequence. The thermodynamic values were calculated from Zuker's Unified Nucleic Acid Folding (UNAFold) program[4] (accessed on 9/16/2014), using 22 °C, 150 mM $Na^+$, and 10 µM oligonucleotide concentration conditions wherever relevant. Bases in the sequences are color coded as follows: thymine (yellow), cytosine (red), adenine (blue), and guanine (green) and bond formation between Watson-Crick base matches and occasional guanine-thymine bases is indicated with a single line between bases.

All chosen aptamers and the DNA probe were of similar base length. All aptamers shared commonalities in their predicted secondary structures (i.e. all possess hairpins as shown in Figure 2.1.1) to allow better comparisons between the samples. Figure 2.1.1 also shows key thermodynamic data for each of the aptamer strands, namely the self melting point for the predicted secondary structures and the Gibbs free energy associated with the intrastrand hybridization of the single-stranded aptamer sequences. All three

aptamer sequences were calculated to stably self fold, indicated by negative Gibbs free energy values; whereas, the DNA probe does not naturally favor self folding at RT. These sequences were selected to specifically evaluate different aspects of the binding interactions. Two VEGF aptamers, **VA1** and **VA2**, were selected for comparison between aptamers for the same non-nucleotide target. A non-VEGF binding aptamer, **AA**, was selected with a similar structure to insure that the binding events observed were specific to aptamer sequences selected for VEGF and not due to nonspecific interactions with an oligonucleotide with a similar intrastrand structure. Finally, the DNA probe, **A20**, was selected to show that bases within linear (i.e. not slef-hybridized) DNA do not induce nonspecific binding of VEGF. **A20** was also a convenient bench mark for the coupling reaction due to its vast prior use in the Milam lab.[3, 5-7]

### 2.1.2 Oligonucleotide and Particle Preparation

Upon arrival all DNA sequences were aliquoted in TRIS-EDTA (TE) buffer. Aliquots were stored at 100 µM concentration at -20 $^{o}$C. Unlabeled (**VA1C**, **NC14**, **DA**) and aminated DNA oligonucleotides (**VA1, VA2**, **AA**, **A20**, **T7**) were stored in pH 7.4 TE, and fluorescein labeled sequences (**VA1C*F**, **VA2C*F**, **B15*F**, **NC18*F**, **NC14*F**) were stored in pH 8.0 TE. The 6-carboxyfluorescein (FAM) label is attached to the 5' end of the oligonucleotide via a three carbon linker. Amine terminal groups (-$NH_2$) are attached to the 5' end using the same 3 carbon linker. Choice of aptamer sequences for VEGF are based on prior work by Hasegawa *et al*.[2] and Battig *et al.*[1] The choice of an aptamer sequence for ampicillin is based on the work of Song *et al*.[8] As stated earlier, the nomenclature is as follows: the two VEGF aptamers are labeled **VA1** and **VA2**; the ampicillin aptamer is labeled **AA**; complementary sequences to a particular aptamer are

denoted with the letter **C** (**VAC1**, **VAC2**, and **AAC**) as well as ***F** if labeled with a FAM moiety. Duplexes are indicated with a colon between sequence names (e.g. **VA1**:**VA1C**). Noncomplementary sequences are denoted by **NC**, their base length, and ***F** to denote the presence of a FAM label. The displacement agent, **DA**, is used to drive release of **VA1C** from **VA1:VA1C** duplexes. In addition to the ampicillin aptamer, **AA**, additional controls are run using a DNA probe, **A20**, along with its 15 base-long complementary sequence, **B15**. Finally, a 7 base-long polythymine sequence, **T7**, is used as a blocking agent to help cap any EDAC-activated sites not occupied by aptamer or probe (in selected cases).

100 µL of (1 µm dia.) carboxylated polystyrene microspheres (1% v/w ) from Bangs Laboratories, Inc. (Fishers, IN) are functionalized with DNA aptamer or probe by adding 200 µL of aminated oligonucleotides (2 µM in Tris-EDTA (TE) pH 7.4) and 25 µL of a 1.0 M concentration of 1-ethyl-3-[3-dimethylaminopropyl]-carbodiimide hydrochloride (EDAC). DNA aptamer or probe coupling to particles was carried out in a similar manner reported previously by the Milam group[6] as schematically represented in Figure 2.1.2.

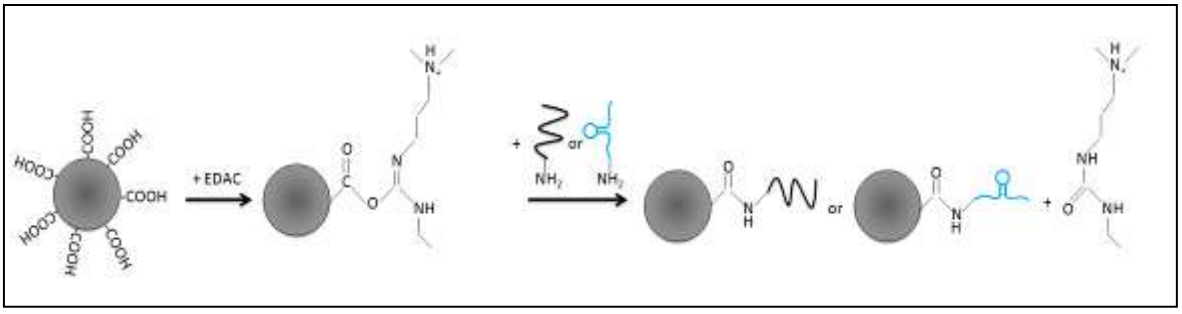


Figure 2.1.2: A schematic diagram illustrating crosslinking of carboxylated microparticles and aminated probe or aptamer sequences, using the carbodiimide molecule, EDAC. For simplicity only a single reaction is shown per particle.

For suspensions involving the blocking agent, **T7**, following a 2 h incubation of either an aptamer species (**VA1**, **VA2**, **AA**) or a probe species (**A20**) with carboxylated

particles in the presence of EDAC, 100 µL of a second shorter, aminated sequence (**T7**, 10 µM in TE pH 7.4) is added to conjugate any remaining EDAC activated sites on the particles and thus act as a "blocking agent" to reduce nonspecific binding events between the particle surface and targets (. Separate studies were carried out using 5 kDa aminated PEG (Sigma Aldrich, St. Louis, MO) as a blocking agent. Following the 1 h incubation with the **T7** sequence or PEG, suspensions were centrifuged (9900g for 5 min) and resuspended in 100 µL of phosphate buffered saline containing 0.2% v/v Tween 20 (PBS/T).

### 2.1.3 Hybridization of DNA-Functionalized Particles and Analysis via Flow Cytometry

Samples for primary hybridization were prepared by taking 2 µL of the final coupling suspension and diluting it to 100 µL using PBS/T, yielding a 0.02 % particles by volume suspension. 100 µL of FITC labeled complementary DNA was prepared in TE pH 8.0 (2 µM) and added to the suspension. The resulting mixture was incubated at room temperature for 8-24 hrs on a rotomixer. Following incubation three washes were performed, centrifuging the samples at 9900xg for 3 min and resuspended in 100 µL PBS/T. The particles were then diluted to 1 mL using PBS/T. The 1 mL suspensions were analyzed on a Becton Dickinson LSR II flow cytometer (Becton Dickinson, San Jose, CA) using FACSDiva software (Beckton Dickinson). Calibration curves was generated using Quantum FITC-5 MESF standards (Bangs Laboratories) and were diluted in the same buffer as the samples, allowing quantification of fluorescence intensity in molecules of equivalent soluble fluorophore (MESF). MESF units from the standards are used to convert the mean fluorescence of each sample to the mean number of dye-labeled targets associated to each particle. Suspensions of EDAC-activated 1 µm PS microspheres, unactivated 1 µm PS beads, and DNA-functionalized 1 µm microspheres incubated with

a noncomplementary target were individually included to verify that binding of FAM-labeled targets is due to specific interactions between complementary DNA sequences.

## 2.2 Results and Discussion

### 2.2.1 Analysis of Primary Hybridization Activity of Soluble Targets

Initially, five sets of particle suspensions (EDAC-activated beads with no immobilized DNA and **A20**, **AA**, **VA1**, and **VA2**-functionalized particles) were prepared to assess the nature of binding of the primary DNA target to the immobilized DNA aptamer and probe sequences. EDAC-activated microspheres were used to assess whether any nonspecific interactions occurred between the labeled DNA sequences and the microsphere's polymeric surface. **A20**, a well known sequence in the Milam group[3, 5-7], was used as a benchmark for the coupling reaction's success since the protocol for this sequence has been previously optimized for DNA binding and release using a displacement agent.[3] The ampicillin aptamer, **AA**, was included in this and later studies to verify that structurally similar aptamer sequences would not nonspecifically bind VEGF, and finally the two VEGF aptamer sequences, **VA1** and **VA2**, were chosen to compare how changes in the binding interactions would affect different aptamers selected for the same non-nucleotide target. Initially, no blocking agent, **T7**, was immobilized on the surface alongside the aptamer sequence. Shown below in Figure 2.2.1 are the observed duplex densities for each of the five bead populations after an 8 h incubation with their respective complementary DNA targets. The inset shows the negative controls in which the five particle populations were each incubated with a noncomplementary FAM-labeled DNA sequence to verify that only complementary sequence interactions dominate the measuremets.

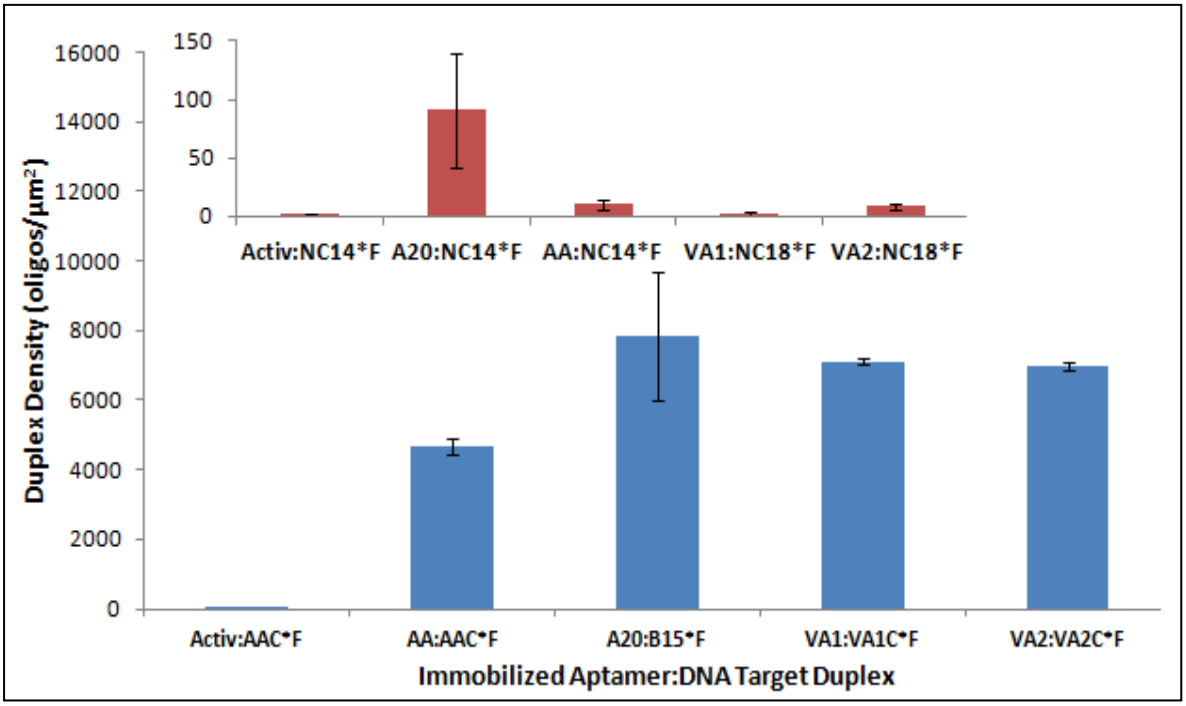


**Figure 2.2.1:**Surface densities of aptamer:DNA target duplexes of various aptamer-functionalized (**VA1**, **VA2**, **AA**) microspheres with their complementary DNA targets (**VA1C**, **VA2C**, **AAC**). EDAC activated microspheres incubated with the **AAC** complementary DNA target is included as an additional control. The inset shows the same populations of aptamer-functionalized particles incubated with noncomplementary DNA targets (**NC14*F** and **NC18*F**) used as a negative control to evaluate the nature of DNA target binding.

The lack of fluorescent signal in the EDAC-activated case and all noncomplementary cases in the inset sharply contrasts to the remaining cases involving complementary sequences. Thus, Figure 2.2.1 indicates that all DNA aptamer and probe sequences were successfully immobilized and able to hybridize on the particle surfaces. Additionally, comparable results were achieved for each of the VEGF aptamer and probe sequences and thus further optimization of the coupling reaction appeared necessary to promote binding of the DNA target.

In an effort to minimize waste of excess aminated DNA, we chose to alter the particle concentration and DNA concentration to assess how much excess DNA was

being used for the coupling reactions. Originally, the standard protocol for EDAC coupling called for 100 µL of 10 µM DNA to yield a suspension containing 1.0 % functionalized particles (v/w). To verify if concentrations could be altered, three particle concentrations were tested: (1) the original concentration 1x (1.0%), (2) one fifth (1/5x) the standard concentration (0.2%), and (3) five times (5x) more concentrated (5.0%). Figure 2.2.2 shows the duplex densities observed when the coupling was performed using these three concentrations. EDAC activated microspheres without immobilized DNA and noncomplementary DNA target controls are also included to show that altering the particle concentration does not promote nonspecific binding. Given the good agreement between the 1x and 1/5x in terms of duplex density values, we chose to reduce the DNA concentration to 2 µM for all future coupling reactions to reduce DNA waste.

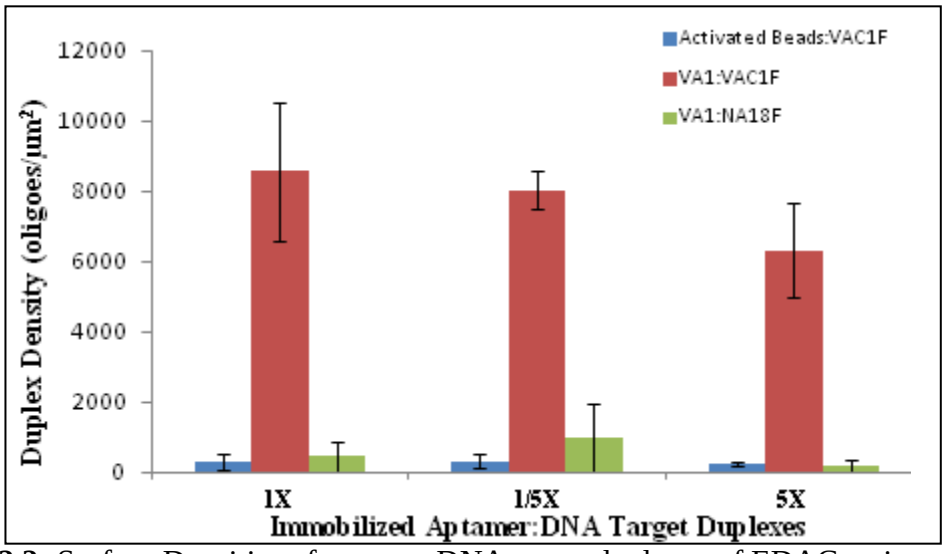


**Figure 2.2.2:** Surface Densities of aptamer:DNA target duplexes of EDAC activated microspheres and **VA1**-functionalized particles and the **VA1C*F** complementary DNA target at various particle concentrations: 1% w/v **(1X)**, 0.2% w/v **(1/5X)**, and 5% w/v **(5X)**.

While the coupling process had now been optimized for specific binding of the primary DNA target, the effects of DNA coupling on non-specific as well as specific binding of the non-nucleotide target, VEGF still require testing. Chapter 3 details these

results for VEGF binding; however, the key effects of these additional modification steps on hybridization of the complementary DNA target are outlined below. As shown in Chapter 3, VEGF was observed to nonspecificallybinding to the microspheres if incubated with microspheres a couple of hours following exposure to EDAC (intended to couple aminated DNA to carboxylated microspheres).. Therefore, we attempted to block off any remaining EDAC moieties on the particles' surfaces through a delayed addition of another aminated macromolecule. Two such molecules were chosen for this purpose: (1) aminated polyethylene glycol (PEG) and an aminated polythymine DNA sequence (**T7**). PEG has been shown previously to sterically hinder nonspecific interactions[9] in biological systems and to promote biostability,[10] making it an excellent candidate to examine for this colloidal system; however, the length of the chosen PEG molecule (5 kDA in MW) could prevent specific interactions as well. **T7** was chosen as an alternative blocking agent candidate since it too should be capable of to any remaining EDAC moieties without impeding interactions of either target molecule, DNA or VEGF, with the aptamer sequence. Which already includes a ten base long thymine spacer ($T_{10}$) next to their immobilized 5' end. Since **T7** is a seven base long polythymine sequence, its short base length should not sterically impede specific interactions (e.g. hybridization as examined here or VEGF binding as examined in Chapter 3). Moreover, its small size should help it penetrate through immobilized aptamers strands to interact with any remaining EDAC moieties.

Figure 2.2.3 shows the results of including PEG or **T7** as a blocking agent on duplex formation. PEG and **T7** were immobilized as described in the experimental section by incubating either aminated PEG or **T7** with the EDAC activated particles

following a wash step after the initial 2 h incubation with the aptamer or probe sequences. As shown by the lower duplex density values in the PEG cases compared to the **T7** cases for **VA1**, PEG significantly hindered the formation of duplexes between the immobilized **VA1** sequence and its complementarty DNA target. These effects were less drastic in the second VEGF aptamer case, VA2; however, subsequent studies focused on the **VA1** system and thus further optimization appeared necessary in the absence of PEG as a blocking agent. Simple calculations of the size of the PEG chain for 5 kDA PEG molecule, using the ideal chain model as outlined in the Appendix showed that the PEG molecule was almost three times the length of the aptamer in its fully elongated state (i.e. not self-folded). Given the relatively larger size of PEG, it may sterically prevent the DNA target from reaching the aptamer sequence, preventing duplex formation. In contrast, **T7** however showed far less of an effect on duplex formation for both VEGF aptamers and was thus selected as a suitable blocking agent for all subsequent experiements.

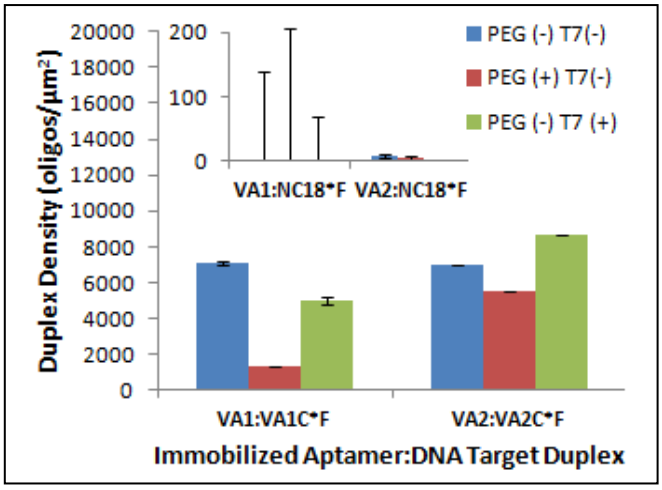


**Figure 2.2.3:** Surface densities of aptamer:DNA target duplexes of VEGF aptamer 1 (**VA1**) and VEGF aptamer 2 (**VA2**) functionalized microspheres in the presence (+) or absence (-) of polyethylene glycol (PEG) or a seven thymine blocking sequence (**T7**) on the microsphere surface as a blocking agent. The controls shown in the inset are for the

same microsphere suspensions and blocking agent conditions; however, incubations involved the noncomplementary DNA target (**NC18**).

Finally, the effect of annealing the aptamer-functionalized particles was evaluated. Theoretically, annealing the aptamer functionalized particles at 60 $^{o}$C it should favor the formation of the predicted intrastrand secondary structures shown in Figure 2.1.1. Many aptamers possess regions of self complementarity which may inhibit hybridization with complementary targets, but could potentially promote homodimer formation (e.g. between two aptamer-functionalized particles) in the absence of complementary DNA. Figure 2.2.4 shows UNAFold predicted structures for homodimer formation between identicle aptamer species. Also included are the Gibbs free energy values for these duplexes.

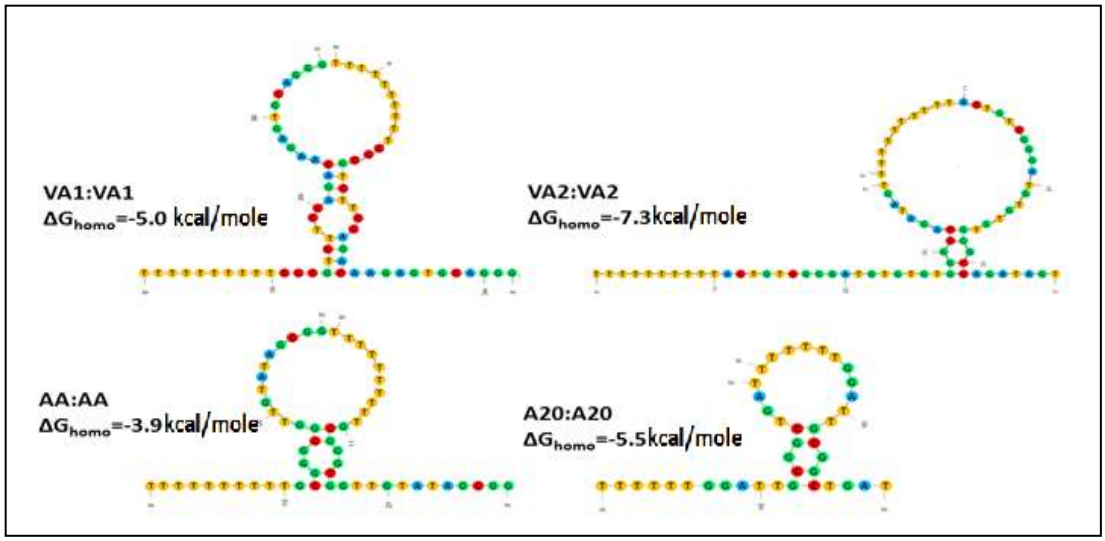


**Figure 2.2.4:** Schematic illustration of homodimer formation between pairs of identical VEGF aptamer 1 (**VA1**), VEGF aptamer 2 (**VA2**), ampicillin aptamer (**AA**), and DNA probe (**A20**) sequences, based on predictions by Zuker's Unified Nucleic Acid Folding (UNAFold) program[4] accessed on 9/16/2014 using 22$^{o}$C, 150 mM $Na^{+}$, and 10 μM oligonucleotide concentration conditions wherever relevant. Bases in sequences are color-coded as follows: thymine (yellow), cytosine (red), adenine (blue), and guanine (green).

Each of the sequences utilized in this work can theoretically form homodimers, as indicated by the negative Gibbs free energy values shown in Figure 2.2.4. These

homodimers, in turn, can lead to aggregation of the colloidal particles. To examine aggregation in aptamer-functionalized microsphers, flow cytometry was utilized. Flow cytometry utilizes forward scatter (FSC) and side scatter (SSC) to cluster populations of similar size and shape. FSC corresponds to the overall size of the particle and SSC gives a measure of the surface complexity of the analyzed particle. Using these values a scatter plot can be generated that separates populations of colloidal particles by size and complexity. Figure 2.2.5(a) shows a scatter plot taken from an early flow cytometry experiments during these optimization attempts for aptamer-functionalized (**VA1**) particles in which three separate populations of particles are gated. These populations correspond to (P1) singlets (individual particles), (P2) doublets (aggregates of two particles), and (P3) multiple-particle aggregates such as triplets. Figure 2.2.5(b) shows **VA1**-functionalized particles following annealing treatment at 60 $^{o}$C. Here, far more particles appear as singlets indicating that annealing appears to reduce aggregation (i.e. increase P1 from 40 % on average (Figure 2.2.5(a) to 85 % on average (Figure 2.2.5(b)), due, most likely, to a reduction in homodimer formation and an increase in the self-hybridized structures in single-stranded aptamers. While this stability in the aptamer-functionalized particles is desirable, we must still test if duplex formation is still favorable in these annealed suspensions. These experiments are discussed next.

Figure 2.2.6 shows the observed duplex densities of **VA1**, **VA2**, and **AA**-functionalized particles if no heat treatment has been performed (no anneal case, **NA**), if the particles were annealed prior (**PA**) to incubation with their DNA target, and if annealed during (**AD**) the first 30 min of the incubation with the primary DNA target. The inset includes noncomplementary controls for each of these types of particles.

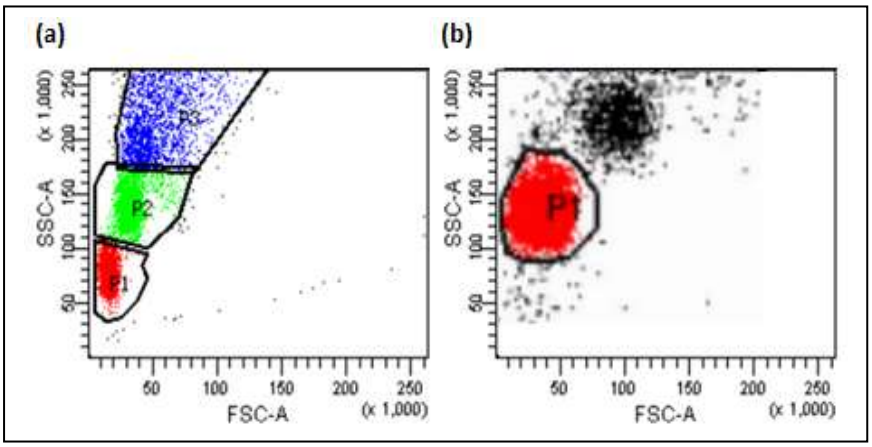


**Figure 2.2.5:** Scatter plots from flow cytometry analysis of **VA1**-functionalized microspheres of forward scatter (FSC-A) vs. side scatter (SSC-A) of annealed aptamer-functionalized (**VA1**) microspheres before (**a**) and after (**b**) the suspensions were annealed. Points shown in the gated P1 population correspond to the singlet population of particles wereas particle clusters are attributed to other gated populations as shown.

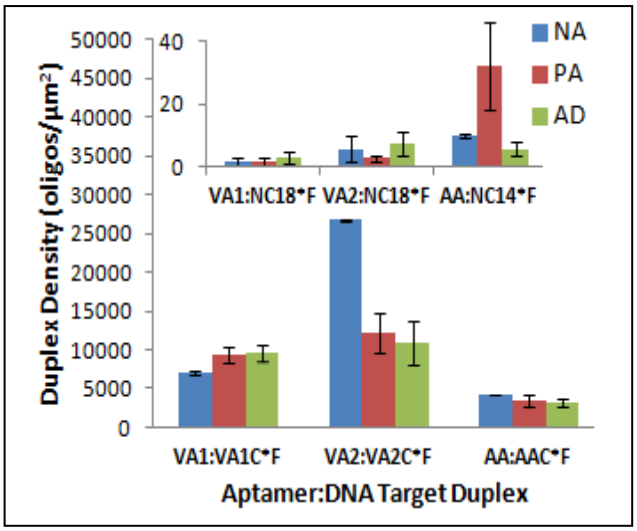


**Figure 2.2.6:** Surface densities of aptamer:DNA target duplexes of various VEGF aptamer 1 (**VA1**), VEGF aptamer 2 (**VA2**), and ampicillin aptamer (**AA**) functionalized microspheres under three annealing conditions: no anneal (**NA**), annealed prior (**PA**) to incubation with the complementary DNA target (**VA1C*F** or **VA2C*F**), and annealed during (**AD**) incubation with the complementary DNA target. The controls shown in the inset contain data for the same microsphere suspensions and annealing conditions; however, incubations involved the noncomplementary DNA target (**NC14** or **NC18**).

As shown in Figure 2.2.6, annealing had various effects on the aptamer:DNA target duplex density values between the aptamers and their complementary DNA targets. For particles functionalized with **VA1** or **AA** the addition of an annealing step only slightly increased the duplex density. In contrast, formation of duplexes with **VA2**-functionalized particles was significantly hindered by adding an annealing step. The stark difference in responses from the two VEGF aptamers may be explained by examining their predicted secondary structures. As seen in Figure 2.1.1, **VA1** and **VA2** both theoretically form a simple hairpin loop structure, but there is one noticeable difference between them. The longer hybridized stem in **VA2** may hinder duplex formation with the complementary DNA target since the DNA target must successfully invade and overcome this self-hybridized stem to form a duplex.

## 2.3 Conclusions

It was shown that binding of the primary DNA target was optimized by decreasing the DNA concentration during the coupling reaction to minimize wasted DNA. Comparable duplex densities to the optimized **A20** DNA probe coupling reaction were achieved, and the inclusion of a blocking agent, **T7**, was shown to not significantly hinder duplex formation, allowing it to be used to optimize VEGF binding events in subsequent studies highlighted in Chapter 3. Heat treatment of aptamer-functionalized microspheres was shown to increase the singlet population, possibly due to favoring formation of the predicted intrastrand secondary structure for the aptamer sequences rather than homodimer formation between opposing aptamer-functionalized particles. These dispersed particles also allow more of the immobilized aptamers available to bind their DNA or non-nucleotide targets. Finally, it was shown that each aptamer may have

to be optimized for future systems incorporating multiple aptamer sequences to achieve multipurpose delivery. This was made apparent when the inclusion of the annealing process significantly hindered binding of the primary DNA target for the second VEGF aptamer sequence (**VA2**), but had little beneficial effect for the first VEGF aptamer-functionalized particles and no discernable effect on the ampicillin aptamer-functionalized particles.

## 2.4 References


1. Battig, M.R., B. Soontornworajit, and Y. Wang, *Programmable Release of Multiple Protein Drugs from Aptamer-Functionalized Hydrogels via Nucleic Acid Hybridization.* J. Am. Chem. Soc., 2012. **134**(30): p. 12410-12413.
2. Hasegawa, H., K. Sode, and K. Ikebukuro, *Selection of DNA aptamers against VEGF(165) using a protein competitor and the aptamer blotting method.* Biotech. Lett., 2008. **30**(5): p. 829-834.
3. Eze, N.A. and V.T. Milam, *Exploring locked nucleic acids as a bio-inspired materials assembly and disassembly tool.* Soft Matter, 2013. **9**(8): p. 2403-2411.
4. Zuker, M., *Mfold web server for nucleic acid folding and hybridization prediction.* Nucleic Acids Res., 2003. **31**(13): p. 3406-3415.
5. Baker, B.A. and V.T. Milam, *Hybridization kinetics between immobilized double-stranded DNA probes and targets containing embedded recognition segments.* Nucleic Acids Res., 2011. **39**(15): p. 13.
6. Tison, C.K. and V.T. Milam, *Reversing DNA-Mediated adhesion at a fixed temperature.* Langmuir, 2007. **23**(19): p. 9728-9736.
7. Tison, C.K. and V.T. Milam, *Programming the kinetics and extent of colloidal disassembly using a DNA trigger.* Soft Matter, 2010. **6**(18): p. 4446-4453.
8. Song, K.M., et al., *Aptasensor for ampicillin using gold nanoparticle based dual fluorescence-colorimetric methods.* Anal. Bioanal. Chem., 2012. **402**(6): p. 2153-2161.
9. Brockman, J.M., A.G. Frutos, and R.M. Corn, *A multistep chemical modification procedure to create DNA arrays on gold surfaces for the study of protein-DNA interactions with surface plasmon resonance imaging.* Journal of the American Chemical Society, 1999. **121**(35): p. 8044-8051.
10. Nahar, M., et al., *Functional polymeric nanoparticles: An efficient and promising tool for active delivery of bioactives.* Critical Reviews in Therapeutic Drug Carrier Systems, 2006. **23**(4): p. 259-318.

# CHAPTER 3

# OPTIMIZING SPECIFC BINDING OF VEGF BINDING TO VEGF APTAMER FUNCTIONALIZED COLLOIDAL PARTICLES

## Introduction

This chapter will detail the experiments to quantify the binding activity of VEGF to aptamer-functionalized microspheres. The initial experiment's focus centers heavily on the steps made to minimize nonspecific binding of VEGF to the EDAC moieties left behind after the aptamer coupling reaction. Outlined within are flow cytometry assays to measure bound VEGF using a multicomponent labeling scheme, and a Luminex-based assay to measure the unbound VEGF remaining in supernatant (following incubation with aptamer-functionalized particles) is also discussed.

### 3.1 Experimental Setup

#### 3.1.1 VEGF Preparation and quantification via Luminex Analysis

10 µg of VEGFA (GeneTex, Inc.) was suspended in phosphate buffer saline containing 0.5 % w/v bovine serum albumin (PBS/BSA). The PBS/BSA was prepared by weighing out 250 mg of BSA and disolving it in 50 mL of PBS. The resulting solution was then denatured using a 60 $^{o}$C water bath over 30 min.[1] The denatured BSA is intended to work in the same manner to help block the particle surface from nonspecific binding of VEGF to the functionalized particles. Luminex analysis was then performed to verify the concentration of VEGF in solution. Using a Luminex cytokine kit (Bio-Rad, Hercules, CA) magnetic beads functionalized with VEGF antibodies were prepared from the supplied stock of beads (10x v/v). The stock beads were vortexed for 30 sec and then 576 µL were added to 5184 µL of the Bio-Plex assay buffer from the kit. The beads were

then vortexed for an additional 30 sec, wrapped in aluminum foil to protect from exposure to ambient light, and allowed to equilibrate to room temperature. 50 µL of the diluted beads were added to each of the wells of a 96 well plate and washed three times with a Bio-Plex Pro Magnetic Wash Station, allowing 60 sec for pelleting to occur, and resuspended in 100 µL of the kit's wash buffer. 50 µL of each sample was then added to the appropriate wells. The plate was covered with parafilm and incubated on a shaker at 850 rpm for 1 hr at room temperature. During the incubation, the Bio-Plex detection antibodies were prepared to label the bound VEGF according to the protocol supplied with the kit, following the equations below.

$$V_{ab} = n * 2.5\ \mu L * 1.25 \qquad (1)$$

$$V_{dilutent} = n * 22.5 * 1.25 \qquad (2)$$

In which $V_{ab}$ is the volume of the stock antibody solution needed, $V_{dilutent}$ is the volume of the antibody dilutent needed, and n is the number of wells used on the plate. The plate was then washed three times, using magnetic separation and the wash buffer supplied with the kit, before being resuspended in 25 µL of the diluted antibody solution and allowed to incubate for 30 minutes. The antibody used was biotinylated, allowing for labeling using a streptavidin associated phycoerythrin (SA-PE) polymer. Following the 30 min incubation, the plate was washed again three times and resuspended in 50 µL of the SA-PE solution, shown in Figure 3.1.1.

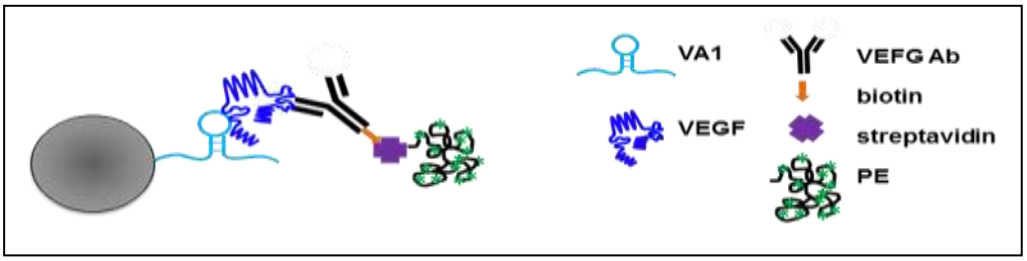


**Figure 1.1.1:** Schematic diagram to illustrate the series of components used to label VEGF bound to its aptamer as shown or bound in a nonspecific manner to an unrelated oligonucleotide or the underlying particles substrate (not shown).

The SA-PE was prepared according to the Bio-Plex protocol using the following equations.

$$V_{SA\text{-}PE} = n * 0.5\ \mu L * 1.25 \qquad (3)$$

$$V_{assay} = n * 49.5\ \mu L * 1.25 \qquad (4)$$

$V_{SA\text{-}PE}$ is the volume of the SA-PE stock solution. $V_{assay}$ is the volume of the assay buffer needed, and n is again the number of wells used in the 96 well plate. A 10 minute incubation is performed at room temperature, and the plate is washed a final three times. The samples are then resuspended in 100 µL of the assay buffer provided in the kit and the Luminex is run. Alongside the VEGF stock solution, a set of cytokine group I standards were run. The standards contain dried preweighed amounts of each of the group I cytokines, including VEGF. The standards are reconstituted in 500 µL of PBS/BSA and lightly vortexed for 5 sec. The vile is then placed in an ice bath for 30 min until ready for dilution. 72 µL of the reconstituted standard are added to 128 µL of PBS/BSA and a 4 fold serial dilution is performed to generate 8 tubes of decreasing concentration. The standards are prepared in the same way as the samples for Luminex and allow for conversion of mean fluorescence intensity to the concentration of VEGF bound to the

particles using a standard curve and fit. All measurements were performed on a Luminex 100/200 system (Luminex Corp, Austin, TX).

### 3.1.2 Preparation of DNA-Functionalized Particles Bound with VEGF Target and Analysis via Flow Cytometry

For the analysis of VEGF binding (shown in Figure 3.1.1), 100 µL of aptamer or probe-functionalized particles (diluted to 0.02% w/v with PBS/T) were first centrifuged (9200g for 5 min) and then resuspended in 100 µL of 0.5% w/v PBS/BSA three times. One of two heat treatments were applied to the aptamer or probe functionalized particles: VEGF was added at room temperature (RT) for 8 h (1) after the DNA aptamer or probe coupling reaction was terminated (no anneal case) or (2) after the suspension was warmed to 60 $^{o}$C for 30 min, then cooled to RT in an HB-1000 hybridizer oven (UPV, LLC, Upland, CA) for 45 min. Notably, annealing aptamer functionalized particles in the absence of any target is intended to favor formation of the predicted intrastrand secondary structure at RT as shown in Figure 2.1.1. For these VEGF binding studies, 100 µL of soluble VEGF (2 µM in PBS/BSA) is incubated with the aptamer or probe-functionalized particles for 8 h. Following incubation, suspension were centrifuged (9900g 5 min) three times and resuspended in 100 µL of PBS/BSA. Then components from the BioPlex Pro Assay kit are added in a sequential manner (per kit instructions) to bound VEGF as illustrated in Figure 3.1.1. In brief, a biotinylated detection antibody that binds to the receptor binding site of the VEGF was added (followed by 3 washes in PBS/BSA), then streptavidin-PE conjugate was added (followed by 3 washes in PBS/BSA).

VEGF binding to DNA-functionalized particles was directly quantified using flow cytometry. Samples were prepared as previously described[2] by diluting the resulting 100 µL suspensions to 1000 µL using PBS/BSA. Conversion of fluorescence intensity values to either Molecules of Equivalent Soluble Fluorophore (MESF) (for bound PE-labeled VEGF) was accomplished using the Quantum R-PE MESF standard (Bangs Laboratories, Fishers, IN) diluted in the 500 µL of PBS/T buffer. All standards and samples were run on a DB LSR II Flow Cytometer (Becton Dickinson, San Jose, CA). BD FACSDiva software was utilized for data acquisition. Samples evaluated included aptamer functionalized particles (1) alone (to measure autofluorescence background) and (2) incubated with VEGF(to measure fluorescence associated with the formation of aptamer:VEGF complexes.

## 3.2 Results and Discussion

### 3.2.1 Analysis of VEGF Binding using Luminex

The Luminex detection system (Luminex Corp, Austin, TX) is a high throughput flow cytometry system built around three core features. First, fluorescently dyed microspheres (Bio-Rad, Hercules, CA) are prepared by the manufacturer to possess a distinct fluorescent color code or spectral address. This permits discrimination between multiple bead types in a multiplex suspension. Second, it utilizes a specific or dedicated flow cytometer with appropriate lasers and optics to measure bound molecules to these specific particles. This point is important since a user cannot emply their own choice of microspheres to directly assess bound species. Instead one uses these specialized beads to capture any remaining species in the supernatant as illustrated in Figure 3.2.1. Thus, one indirectly assesses the amount of bound species in their own suspensions by analyzing

the supernatant with these specialized beads.Third, the system has a high speed processor for managing the accumulated fluorescence data. This setup allows for rapid simultaneous analysis of complex systems containing more than 100 different bead types.[3] Using a Bio-Rad kit designed for VEGF, Luminex analysis was performed on the VEGF stock solution (to provide a calibration curve) and then on the VEGF remaining in suspension following incubation with aptamer functionalized beads (shown in Figure 3.2.1).

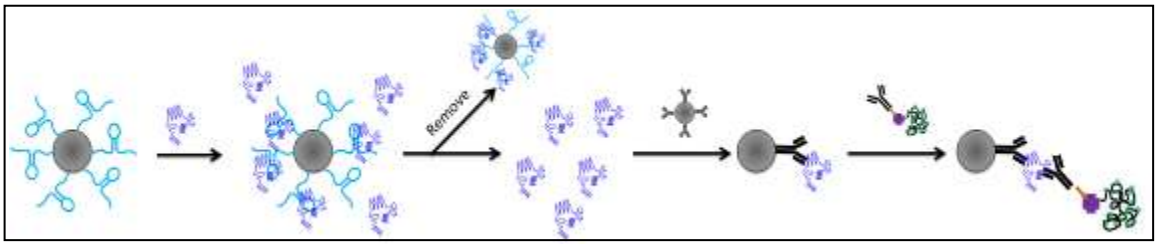


Figure 3.2.1: A schematic representation outlining the preparatory steps for capture and analysis of VEGF remaining in solution for the Luminex. Following incubation with the aptamer-functionalized microspheres, VEGF molecules remaining in solution are incubated with magnetic particles functionalized with VEGF antibodies. Then a series of labeling components, including a second soluble biotinylated VEGF antibody and a streptavidin associated PE molecule are incubated with magnetic particles to tag any antibody bound VEGF.

Figure 3.2.2 shows the results from a calibration standard (Bio-Rad, Hercules, CA) prepared for human group I cytokines, including VEGF. A premeasured amount of VEGF was dissolved within PBS/BSA to prepare the initial standard and 4-fold dilutions were executed to measure the fluorescence intensity associated with five known concentrations to generate the calibration shown in Figure 3.2.2(a). Trend lines were applied to the full eight point standard curve and to the 4 points, corresponding to the lowest concentration standards. This was done to insure a better fit at the four lower concentrations shown in Figure 3.2.2(b).

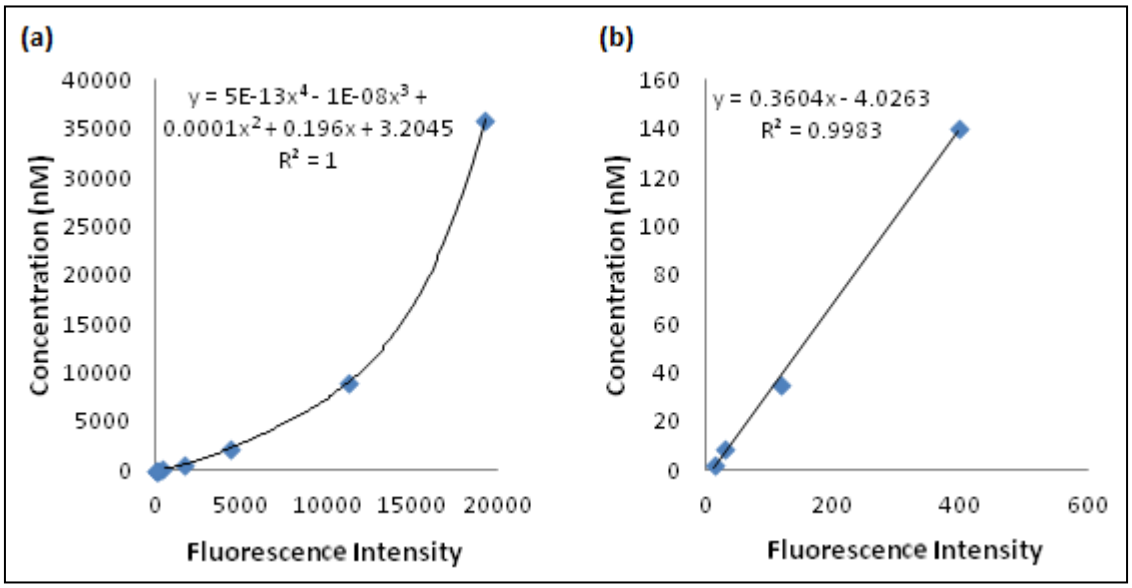


**Figure 3.2.2** Calibration curve for VEGF concentration generated using the Bio-Plex Pro Human Cytokine Standard 27-Plex, Group I from Bio-Rad. (**a**) The full curve for all 8 standards prepared using serial dilution as per kit instructions. (**b**) The four lowest concentrations are shown to establish a linear relationship between concentration and fluorescence intensity.

Table 3.2.1 shows raw data used to create the calibration curves shown in Figure 3.2.2. Standards were prepared from a reconstituted vial containing measured amount of human group 1 cytokines. A fourfold dilution was performed between each standard, using PBS/BSA, according to the kit's protocol. Also listed in Table 3.2.1 is the fluorescent intensity across 50 randomly samples particles in suspension by the luminex system, the expected concentrations of VEGF for each standard based on the initial concentration of VEGF in standard S1, and the concentrations calculated using the generated calibration curves shown in Figure 3.2.2.

**Table 3.2.1:** Standard data from the luminex analysis of Human Cytokine Group 1Standards from Bio-Rad for the Bio-Plex system, using a fourfold serially diluted reconstituted standard containing a measured amount of VEGF and other cytokines. List are the standards designation number during serial dilution, the mean fluorescent intenstity measured by the Bio-Plex system, the expected concentration of VEGF in each dilution based on the original weighed amount of VEGF present in standard S1, and the calculated concentration from the generated calibration curves.

| Standard | Mean Fluorescent Intensity | Actual Concentration (M) | Calculated Concentration (M) |
|---|---|---|---|
| S 1 | 19239 | 3.59E-05 | 3.82E-05 |
| S 2 | 11232 | 8.97E-06 | 8.71E-06 |
| S 3 | 4284 | 2.24E-06 | 2.10E-06 |
| S 4 | 1589 | 5.6E-07 | 5.51E-07 |
| S 5 | 397 | 1.4E-07 | 1.39E-07 |
| S 6 | 119 | 3.5E-08 | 3.89E-08 |
| S 7 | 31 | 8.76E-09 | 7.03E-09 |
| S 8 | 14 | 2.19E-09 | 1.02E-09 |

Using the calibration curve we then attempted to measure the amount of VEGF bound to aptamer functionalized particles. As outlined above, samples were prepared, allowing VEGF to incubate with the aptamer functionalized particles for 8 hrs prior to beginning the luminex study. Samples were prepared using pM concnetrations of VEGF based on estimates of amount of aptamer available for binding VEGF. To estimate the amount of aptamer and VEGF, we used the primary hybridization duplex density previously reported in Figure 2.2.2 and assumed the aptamer-to-bound VEGF ratio. The system was designed for 50 % binding of VEGF initially, to create an easily detectible change in VEGF supernatant concentration because the luminex was used to examine the VEGF that did not bind and was left behind after washing and removing the supernatant from the beads (Figure 3.2.1). Other groups had previously reported being able to measure concentrations in the pM range, but we were not able to distinguish between solutions without any VEGF present and the stock VEGF solution (12.11 pM), as shown in Figure 3.2.3.

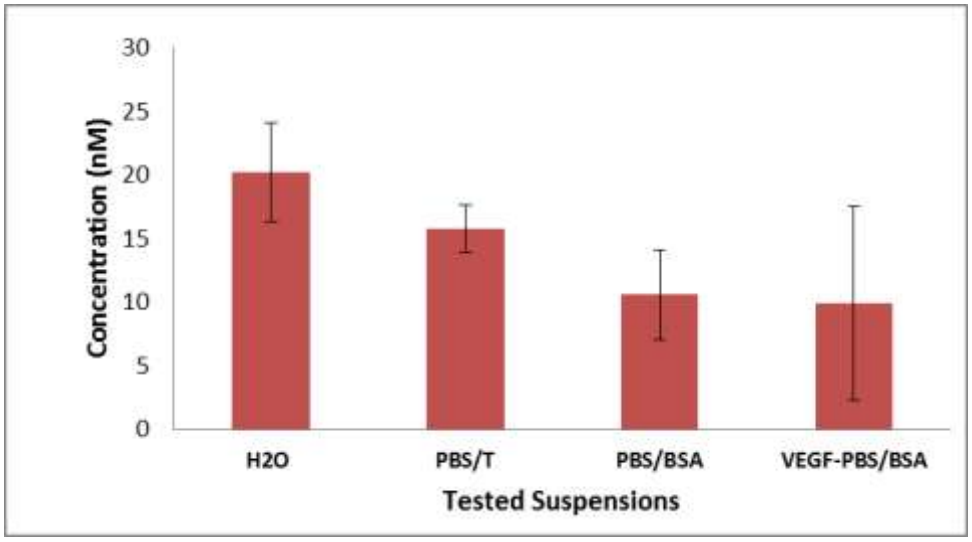


**Figure 3.2.3** Concentrations of VEGF in solution converted from the measured average fluorescent intensity for $H_2O$, PBS/T, PBS/BSA, and a 12.11 pM VEGF stock solution using the Luminex kit from Bio-Rad. $H_2O$, PBS/T, PBS/BSA were samples without VEGF present in solution.

A reoptimization was attempted for nM concentrations of VEGF, since the standards showed better fidelity between the calculated and expected concentrations within this range. Figure 3.2.4 shows the results from this reoptimization. Both trend lines shown above were used in calculating the concentrations, and the calculation based off the lower four points is denoted as low conc and shown in red. Despite reoptimizing the system for the higher concentrations, the experiment failed, showing no binding for both the VEGF aptamer (**VA1)** and the negative control, ampicillin aptamer (**AA**). Any further changes the the experiment would have required working with multiple milliliters of coupled beads, a costly and time consuming experiment, so the Luminex study was forgone and an alternate analysis technique was used, involving the luminex labeling kit and a BD LSR II flow cytometer.

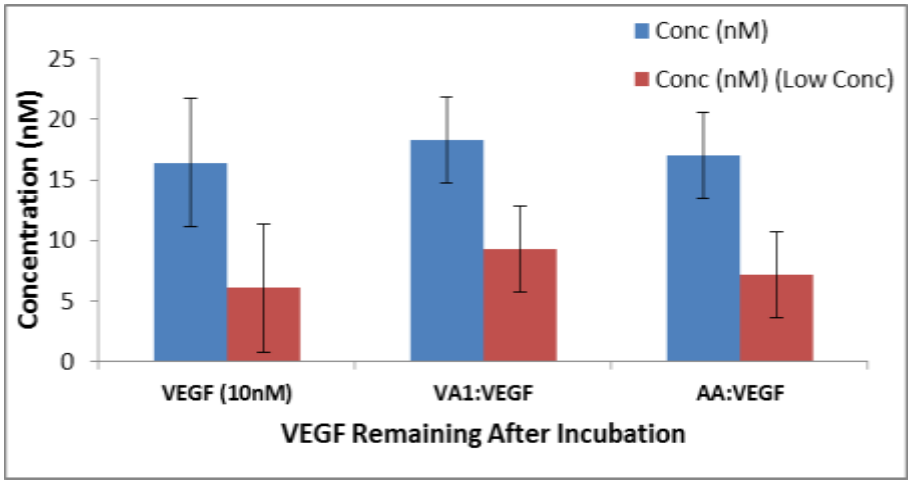


**Figure 3.2.4** Converted VEGF concentrations using the Luminex instrument. Analysis was performed on the VEGF remaining in supernatant following incubation with the indicated aptamer functionalized beads and compared to the stock 10 nM VEGF solution.

### 3.2.2 Analysis of VEGF Binding using Flow Cytometry

Flow cytometry was used as an alternate to measure relative amounts of bound VEGF. Notably, no calibration standards are available for converting fluorescence intensity values tino amounts of bound VEGF due to the polymeric nature of the PE label (with multiple dye molecules). $VEGF_{165}$ the major isoform of VEGF, possesses two binding sites: a heparin binding domain and a cell receptor binding domain.[4, 5] The two VEGF aptamers used in this work reportedly to bind to the herapin binding domain, leaving the receptor binding domain free to be accessed by the biotinylated detection antibody from the luminex kit.[5, 6] The kit was optimized for a 1.0 % population of aptamer-functionalized microspheres. A more concentrated microsphere volume was employed than what is typically used for flow cytometry according to enable use of the Luminex kit to label the aptamer-bound VEGF for flow cytometry. Figure 3.2.5 shows the results from the initial trial of the labeling process for flow cytometry. Three different concentrations of VEGF were analyzed to determine if a detection limit existed for this labeling technique: 10 µM, 10 nM, and 10 pM. No binding was detected for the nM and

pM concentrations, but a significant amount of binding was observed of the 10 µM case, as indicate by the nonzero MESF value associated with PE-labeled bound VEGF.

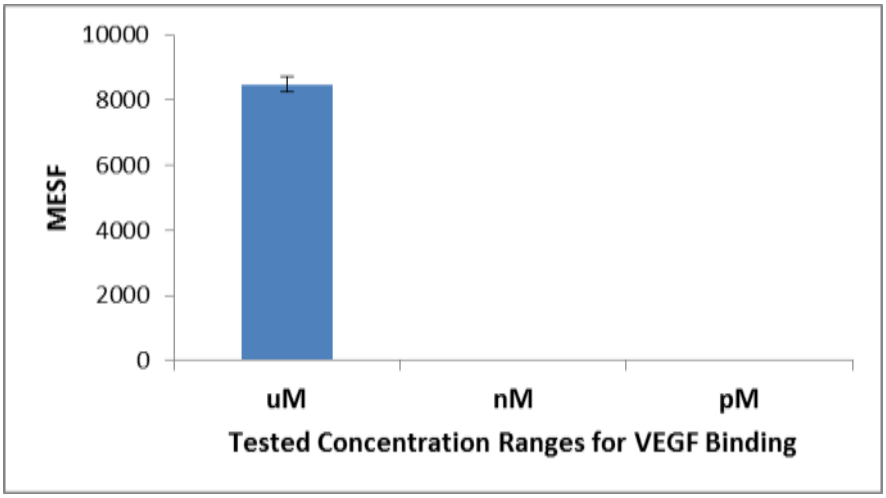


**Figure 3.2.5** Molecules of equivalent soluble fluorophore MESF associated with PE-labeled VEGF bound to immobilized **VA1** at three concentrations of VEGF: (1) 10 µM, 10 nM, and 10 pM

Now that the 10 µM detection limit has been established to quantify bound VGEF (whether specific or nonspecific) using flow cytometry, it was now necessary to minimize any nonspecific binding of VEGF. VEGF binding to the aptamer-functionalized microspheres without the **T7** blocking sequence was analyzed next. Significant VEGF binding was observed (Figure 3.2.6) for the **A20**, **AA**, and EDAC activated 1 µm PS particles in the absence of **T7**. Though more VEGF binding was observed for the **VA1** case, it is evident that nonspecific binding is significant in these suspensions. There was one exception to the outcome. The lack of any fluorescence associated with VEGF bound to the unactivated (i.e. carboxylated) beads indicates that one source of nonspecific interactions could be the EDAC moeities left behind after aptamer coupling. EDAC reportedly has a short lifespan in solution[7] but appears to remain active on the particle surface after converting the carboxyl functional groups to

intermediates. This fact was confirmed in separate experiments to be discussed in Figure 3.2.7. The **T7** blocking agent was introduced in an attempt to exhaust these moeitites.

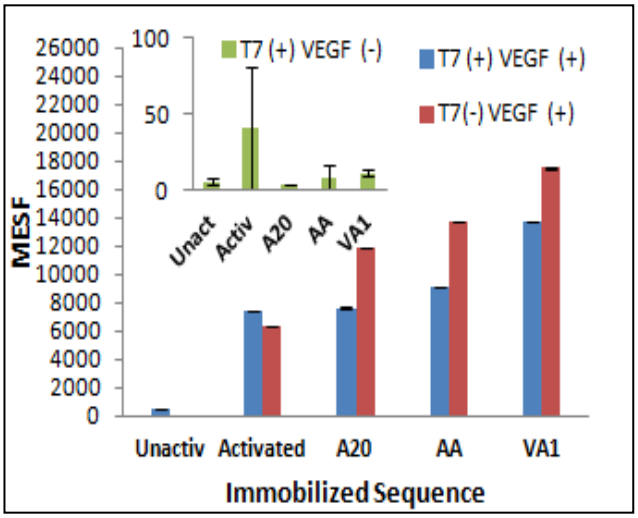


**Figure 3.2.6:** Molecules of Equivalent Soluble Fluorophore (MESF) measured from phycoerythrin (PE) labeled VEGF bound to various bare (unactivated), EDAC incubated (Activated), and DNA (**A20**, **AA**, and **VA1**) functionalized microspheres in the absence (**T7**(-)) or presence (**T7**(+)) of a short, seven thymine blocking agent. Controls shown in the inset show the same microsphere suspensions incubated with PE label, but in the absence of any VEGF.

As shown in Figure 3.2.6, the amount of fluorescence associated with VEGF binding decreases in every DNA-functionalized suspension case. Thus, incorporation of the **T7** blocking sequence appears to serve to reduce but not elminate nonspecific binding Having confirmed the partial success of the **T7** blocking agent, we decided to test the lifespan of EDAC on the particle surface. To accomplish this, the coupling reaction was repeated, but DNA was introduced to the solution at different time points (0-4 h) after the particles had been exposed to EDAC. The first three time points (0-2 h) correspond to the length of the standard coupling protocol with the first aminated DNA sequence (e.g. aptamer). The 2 h timepoint corresponds to the introduction of the aminated **T7** sequence. The fourth time point (3 h) corresponds to the end of the blocking agent's incubation with the particles, and the final time point (4 h) is used to establish if the EDAC moieties

remain active, even after all aptamer and blocking agent incubation periods. Figure 3.2.7 shows the significant duplex densities achieved with the delayed additions of aminated sequence results from this study, indicating that EDAC moieties remain active for over 4 hours despite the reported short lifetime of EDAC.

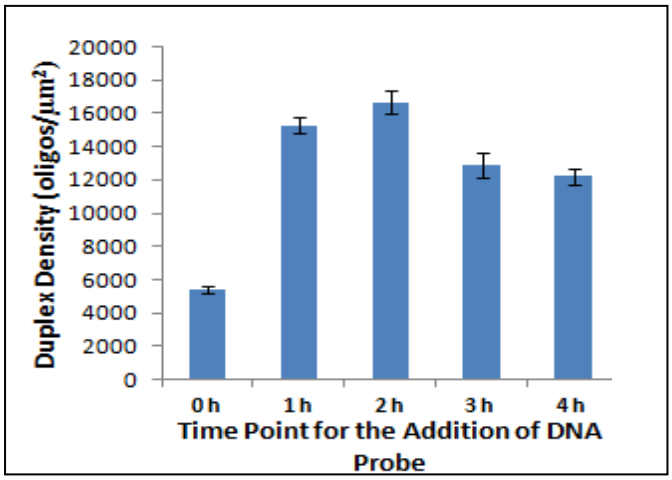


**Figure 3.2.7:** Surface densities of the ampicillin aptamer:DNA target duplexes following incubation with FAM-Labeled complementary DNA target (**AA**:**AAC*F**). The aptamer (probe) sequences were introduced to the EDAC activated particles at the 0, 1, 2, 3, and 4 h time points to evaluate EDAC viability over time.

In light of these time studies with EDAC and delayed addition of aminated DNA that still effectively coupled to the particles, concerns that amine groups on VEGF could couple to any remaining EDAC moieties on the aptamer-funcionalized particles were raised. To examine the combinded effect of including the T7 blocking agent as well as an overnight aging step prior to VEGF addition, all future samples were aged for 8 hrs overnight to further exhaust the lifespan of the EDAC moieties. Particles functionalized with **VA1**, **VA2**, or **AA** were prepared aged before they were incubated with VEGF. Figure 3.2.8 shows the results of this study and shows significant fluorescence due to VEGF binding occuring only in the two VEGF aptamer cases, and not in the negative controls involving the ampicillin aptamer.

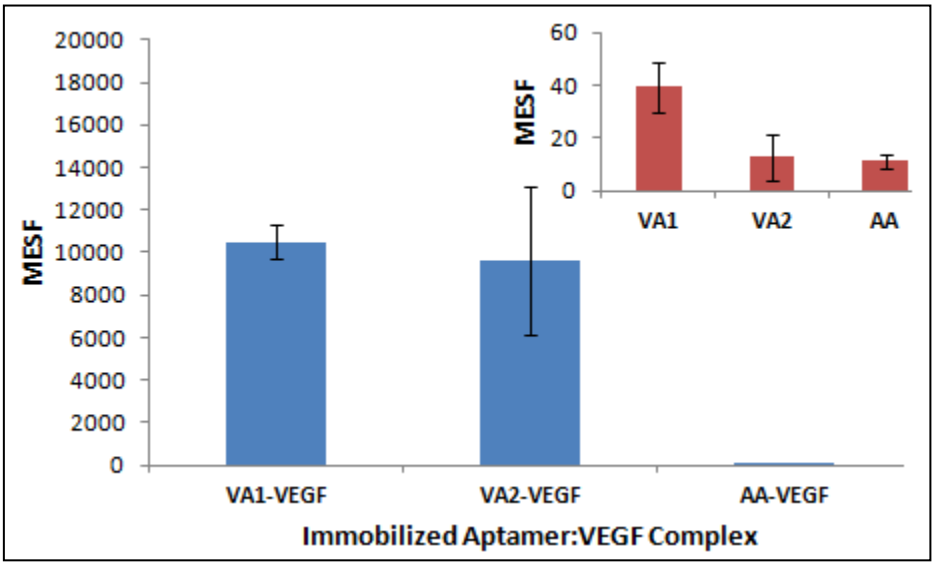


**Figure 3.2.8:** Molecules of Equivalent Soluble Fluorophore (MESF) measured from phycoerythrin (PE) labeled VEGF bound to VEGF Aptamer 1 (**VA1**) , VEGF Aptamer 2 (VA2) and ampicillin aptamer (**AA**) functionalized microspheres 8 h after the completion of the coupling reaction. Controls shown in the inset show the same microsphere suspensions incubated with the PE label in the absence of any VEGF.

As an added control shown in the inset of Figure 3.2.8, samples that were unexposed to VEGF but otherwise were exposed to the full labeling steps to verify that labeling components themselves do not bind to particles in the absence of VEGF. No fluorescence was observed in these controls, indicating that the observed fluorescence can be attributed to labelling components binding only to VEGF itself.

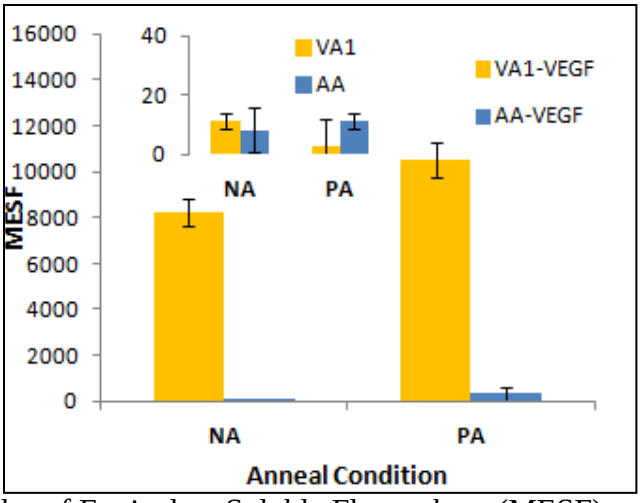


**Figure 3.2.9:** Molecules of Equivalent Soluble Fluorophore (MESF) measured from phycoerythrin (PE) labeled VEGF bound to VEGF Aptamer 1 (**VA1**) and ampicillin aptamer (**AA**) functionalized microspheres under two annealing conditions: no anneal (**NA**) and annealed prior to VEGF incubation (**PA**). Controls shown in the inset show the same microsphere suspensions incubated with the PE label in the absence of any VEGF.

Finally, the effects of annealing on VEGF binding were examined. Without the extra annealing step, these particles were more prone to aggregation possibly due to interparticle interactions between homodimers of the immobilized aptamer sequences (FIgure 2.2.5). Additionally, VEGF binding itself may require the aptamer to adopt its single stranded secondary structure.[8, 9] The anneal should favor the formation of the stem and loop structure predicted by the UNAFold[10] webserver and shown in Figure 2.1.1. Annealing the functionalized beads prior to introduction fo the VEGF solution did show a noticeable increase in binding for the VEGF aptamer case, but not to ampicillin aptamer-functionalized particles. Thus annealing the VA1-functionalized particles appears to further enhance only specific bidning of VEGF as shown in Figure 3.2.9.

## 3.3 Conclusions

Binding of the non-nucloetide target, VEGF, to the aptamer-functionalized particles was optimized by minimizing nonspecific binding and maximizing specific interactions between the aptamers and the protein. Nonspecific interactions were

minimized by incorporating a blocking agent, **T7**, into the coupling reaction. This aminated sequence further exhausted remaining EDAC moieties on the particle surface, but it was also necessary to age the particles for a minimum of 8 h to significantly eliminate nonspecific interactions. Finally, specific interactions were enhanced by annealing the aptamer-functionalized particles. This annealing process likely favors the formation of singlet populations of dispersed VA1 aptamer-functionalized particles and self folding of the aptamers into their predicted single stranded secondary structures.

### 3.4 References


1. Takeda, K., et al., *Conformational change of bovine serum albumin by heat treatment.* Journal of Protein Chemistry, 1989. **8**(5): p. 653-659.
2. Eze, N.A. and V.T. Milam, *Exploring locked nucleic acids as a bio-inspired materials assembly and disassembly tool.* Soft Matter, 2013. **9**(8): p. 2403-2411.
3. Diaz, M.R., et al., *Molecular detection of harmful algal blooms (HABs) using locked nucleic acids and bead array technology.* Limnology and Oceanography-Methods, 2010. **8**: p. 269-284.
4. Ferrara, N. and T. DavisSmyth, *The biology of vascular endothelial growth factor.* Endocrine Rev., 1997. **18**(1): p. 4-25.
5. Potty, A.S.R., et al., *Biophysical Characterization of DNA Aptamer Interactions with Vascular Endothelial Growth Factor.* Biopoly., 2009. **91**(2): p. 145-156.
6. Hasegawa, H., K. Sode, and K. Ikebukuro, *Selection of DNA aptamers against VEGF(165) using a protein competitor and the aptamer blotting method.* Biotech. Lett., 2008. **30**(5): p. 829-834.
7. Hermanson, G.T., *Chapter 5 - Heterobifunctional Crosslinkers*, in *Bioconjugate Techniques (Second Edition)*, G.T. Hermanson, Editor. 2008, Academic Press: New York. p. 276-335.
8. Battig, M.R., B. Soontornworajit, and Y. Wang, *Programmable Release of Multiple Protein Drugs from Aptamer-Functionalized Hydrogels via Nucleic Acid Hybridization.* J. Am. Chem. Soc., 2012. **134**(30): p. 12410-12413.
9. Jayasena, S.D., *Aptamers: An emerging class of molecules that rival antibodies in diagnostics.* Clin. Chem., 1999. **45**(9): p. 1628-1650.
10. Zuker, M., *Mfold web server for nucleic acid folding and hybridization prediction.* Nucleic Acids Res., 2003. **31**(13): p. 3406-3415.

# CHAPTER 4

# COMPETITIVE BINDING OF VEGF AND COMPLEMENTARY DNA TO APTAMER FUNCTIONALIZED COLLOIDAL PARTICLES

## Introduction

This chapter focuses on the studies investigating the dual nature of aptamer binding. Aptamer-functionalized particles are coincubated with both primary targets, DNA and VEGF, or serially incubated with the two targets. Samples are prepared using one of three heat treatments: no anneal (**NA**), using the coupled beads after aging for 8 hrs; preannealed (**PA**), where the particles are brought to 60 $^{o}$C and cooled to room temperature (RT) before incubation of either primary target; and annealed during (AD), where the samples are taken to 60 $^{o}$C for 30 min with the complementary DNA present in solution and then allowed to cool naturally to room temperature over the remainder of the incubation. There are three key studies included within this chapter: the effects of hybridization on VEGF binding activity, the effects of VEGF binding on hybridization, and the effects of coincubating equal concentrations of DNA and VEGF introduced to the aptamer functionalized particles together.

## 4.1 Experimental Setup

### 4.1.1 Competitive Binding and Displacement Sample Preparation

Upon completion of the functionalization of the microspheres with the aptamer or probe and blocking agent, suspension were heat-treated (described in the next paragraph) and then incubated with either its VEGF target (see Figure 4.1.1a), its DNA target (see Scheme 4.1.1d) or both (see Scheme 4.1.1c).

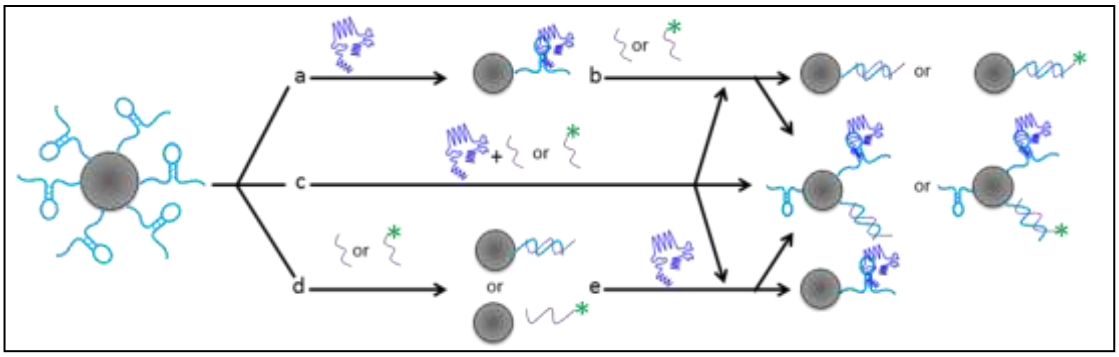


**Figure 4.1.1:** Illustration of aptamer-mediated binding of VEGF and/or DNA targets. Aptamer-functionalized microspheres are incubated with (a) VEGF alone and then (b) unlabeled or labeled DNA target; (c) VEGF and unlabeled or labeled DNA target simultaneously; (d) unlabeled or labeled DNA target alone and then (e) VEGF.

For the analysis of VEGF binding (shown in Scheme 4.1.1a), 100 µL of aptamer or probe-functionalized particles (diluted to 0.01% w/v) were first centrifuged (9200g for 5 min) and then resuspended in 100 µL of 0.5% w/v PBS/BSA three times. One of two heat treatments were applied to the aptamer or probe functionalized particles: VEGF was added at room temperature (RT) for 8 h (1) after the DNA aptamer or probe coupling reaction was terminated (no anneal case) or (2) after the suspension was warmed to 60 $^{o}$C for 30 min, then cooled to RT in an HB-1000 hybridizer oven (UPV, LLC, Upland, CA) for 45 min. Notably, annealing aptamer functionalized particles in the absence of any target is intended to favor formation of the predicted intrastrand secondary structure at RT as shown in Figure 2.1.1. For these VEGF binding studies, 100 µL of soluble VEGF (2 µM in PBS/BSA) is incubated with the aptamer or probe-functionalized particles for 8 h. Following incubation, suspension were centrifuged (9900g for 5 min) three time and resuspended in 100 µL of PBS/BSA. Then components from the Bio-Plex Pro Assay kit are added in a sequential manner (per kit instructions) to bound VEGF as illustrated in Figure 4.1.2 In brief, a biotinylated detection antibody that binds to the receptor binding

site of the VEGF was added (followed by 3 washes in PBS/BSA), then streptavidin-PE conjugate was added (followed by 3 washes in PBS/BSA).

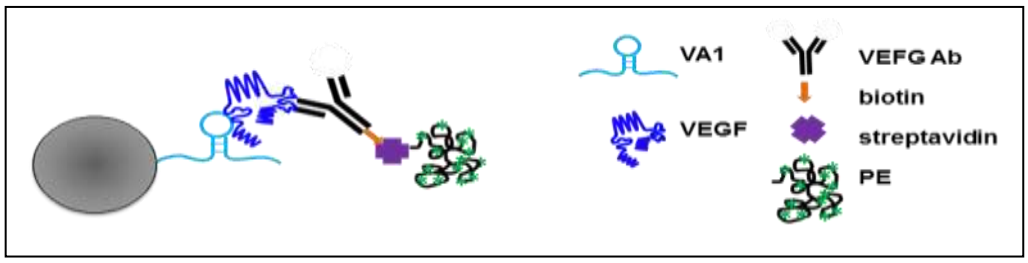


**Figure 4.1.2:** Schematic diagram to illustrate the series of components used to label VEGF bound to its aptamer as shown or bound in a nonspecific manner to an unrelated oligonucleotide or the underlying particles substrate (not shown).

Samples for hybridization of the primary DNA target, shown in Scheme 4.1.1d, were prepared by adding 100 µL of FAM-labeled DNA target at 2 µM to 100 µL of aptamer or probe-functionalized particles (0.1% w/v) for 8 h at RT. Following incubation with DNA target samples were washed by centrifugation (9900g 3 min) and resuspended in 100 µL PBS/T three times.

Coincubation of primary targets was performed using equal concentrations (2 µM) of the FAM-labeled DNA and VEGF targets as shown in Scheme 4.1.1c. 100 µL of the DNA and VEGF suspension were added to 100 µL of 0.1% w/v of DNA-functionalized particles for 8 h. Following incubation three washes were performed by centrifuging the particles (9900g 3 min) and resuspending the particles in 100 µL of PBS/BSA. Samples for the analysis of the effects of serial incubation of both primary targets were prepared using the appropriate heat treatment as described above and then incubated with either VEGF or the complementary DNA for 8 h as previously described. Following the initial incubation three washes were performed by centrifuging (9900g 5 min) the suspensions and resuspending the pellet in 100 µL of PBS/T then incubating

with FAM-labeled DNA (100 µL at 2 µM in TE pH 8.0) second or 100 µL PBS/BSA when incubating with VEGF (100µL at 2 µM in PBS/BSA) second. The second target, as shown in Scheme 4.1.1b and 4.1.1e, is then added to the suspension for 8 h.

All samples were prepared for analysis using flow cytometry as previously described by the Milam lab.[1] The particle suspensions were diluted to 1 mL using PBS/T following three washes (centrifugation at 9900xg for 3 min and resuspended in 100µL PBS/T) . The 1 mL suspensions were analyzed on a Becton Dickinson LSR II flow cytometer (Becton Dickinson, San Jose, CA) using FACSDiva software (Beckton Dickinson). Calibration curves was generated using Quantum FITC-5 MESF standards (Bangs Laboratories, Fishers, IN) or Quantum R-PE MESF standard (Bangs Laboratories, Fishers, IN) and were diluted in the same buffer as the samples, allowing quantification of fluorescence intensity in molecules of equivalent soluble fluorophore (MESF). MESF units from the standards are used to convert the mean fluorescence of each sample to the mean number of targets associated to each particle. For suspensions of EDAC-activated 1 µm PS beads, unactivated 1 µm PS beads, and DNA functionalized beads mixed with a noncomplementary target were included to verify that all hybridization corresponds to specific interactions between complementary DNA sequences.

## 4.2 Results and Discussion

### 4.2.1 Analysis of the Effects of Coincubation and Serial Incubation on the Binding of the Primary Targets

With nonspecific interactions minimized for the colloidal system, the next step was to evaluate the interplay between the two targets. **VA1** has previously been included in a triggered release system by Battig *et al.*[2]However, that system had the aptamer

sequences embedded inside a water swelled hydrogel matrix and focused on characterizing the release of the target protein molecules. Instead, we discuss directly measuring the amount of bound target to particle-immobilized aptamer sequences. To accomplish this we (1) individually incubated one type of particle; (2) coincubated the VEGF and DNA targets with each of the aptamer-functionalized particles (**VA1**, **VA2**, **AA)** for 8 h or, (3) serially incubated the aptamer-functionalized particles with each target. Results for incubation of the two VEGF aptamers (**VA1** and **VA2**) with their labeled complementary sequence shown below in Figure 4.2.1.

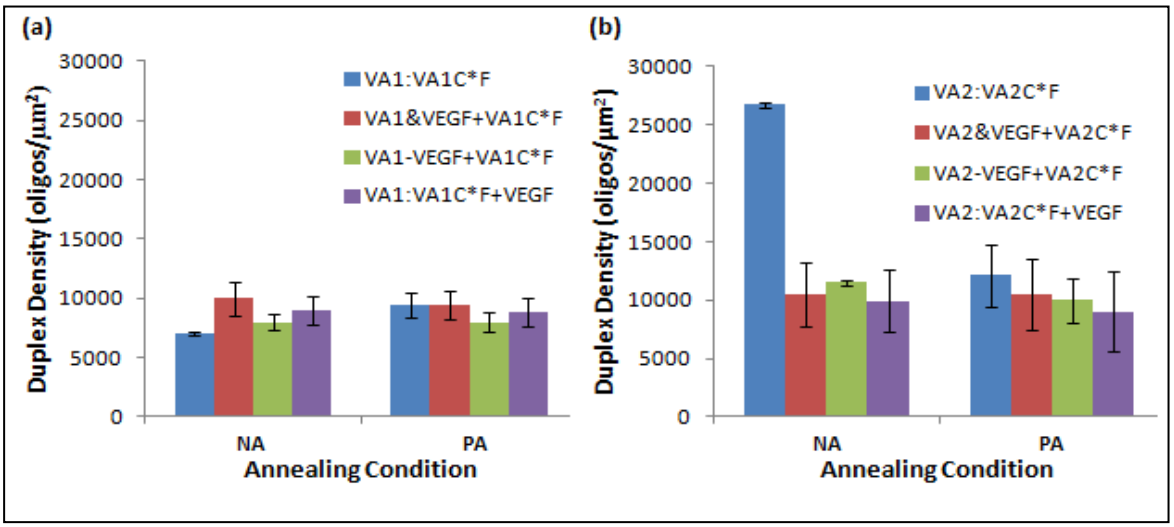


**Figure 4.2.1:** Surface densities of aptamer:DNA target duplexes of (a) VEGF aptamer 1 (**VA1**) and (b) VEGF aptamer 2 (**VA2**) functionalized microspheres following incubation with only the FITC-labeled complementary target (**VA1C*F** or **VA2C*F**) (blue); incubated simultaneously with equivalent concentrations of the DNA target and VEGF (red); incubated first with VEGF and then with the complementary target (green), and incubated with the DNA target first and VEGF second (purple) under two annealing conditions: no anneal (**NA**), annealed prior (**PA**) to incubation with any target (DNA or VEGF).

The presence of VEGF prior, during, or following hybridization had little effect on duplex density values for in particles functionalized with **VA1** as shown in Figure 4.2.1. This trend held true even when the suspensions were heat treated to favor the

formation of the predicted self folded secondary structure in the aptamers. This result indicates that the primary DNA target may serve as a suitable trigger for VEGF release, but it is important to remember that it is unlikely that the immobilized aptamers are fully saturated with VEGF and/or DNA as the initial target. In particular, the fact that the coincubation showed similar duplex densities does indicate that the aptamer may possess a higher affinity for the DNA target than for VEGF. It should be noted that these conclusions cannot be drawn from this one study since VEGF is not labeled in these studies.

The results for **VA2-**functionalized particles shows a much different trend. Coincubation or serial incubation with VEGF severely hindered duplex formation for these particles. This result is especially true for the serial incubation of particles functionalized with **VA2** where the complementary DNA target was first incubated with the aptamer-functionalized particles, resulting in a large decrease in the observed duplex density when compared to the duplex density when only the DNA target is incubated with the particles. This result could potentially arise from VEGF directly interfering with the formation of **VA2**:DNA target duplexes. Therefore, it is possible that this **VA2** aptamer possesses a higher affinity for its protein target and VEGF is capable of displacing this complementary DNA target. For the goals of this project, this combination of VEGF and DNA target may not allow for DNA-triggered release of bound VEGF. Future work would entail using a long DNA target with a higher affinity for the aptamer and provide better prospects as a displacement agent for VEGF.

Figure 4.2.2 shows the negative controls for the coincubation and serial incubation studies of the two VEGF aptamers: **VA1** (a) and **VA2** (b) shown in Figure

4.2.1. Samples were prepared as previously described, but a noncomplementary FAM-labeled DNA sequence was used in place of the FAM-labeled DNA target. Negligible duplex densities were observed for all samples indicating that nonspecific binding did not occur due to the inclusion of VEGF in these studies.

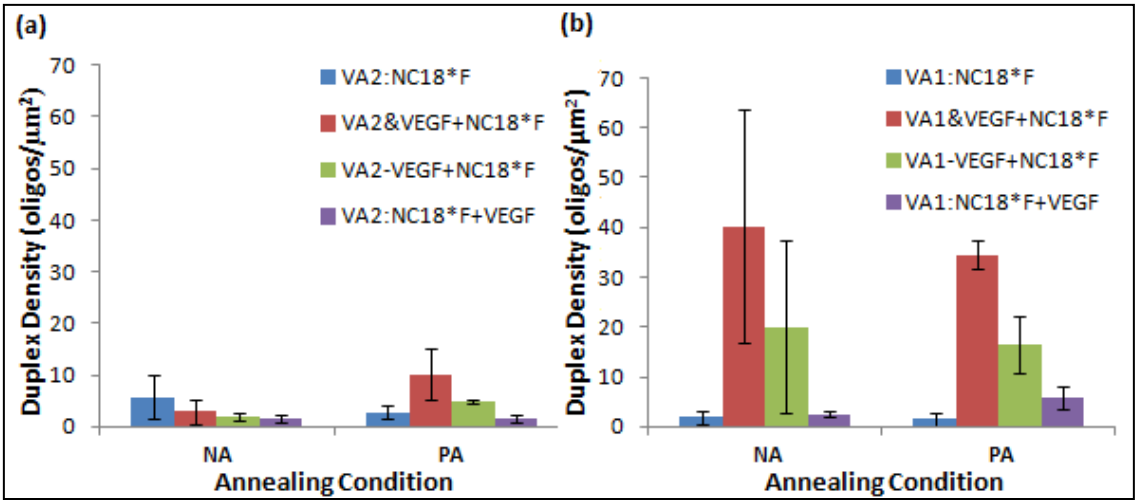


**Figure 4.2.2:** Surface densities of (a) VEGF aptamer 1 (**VA1**) and (b) VEGF aptamer 2 (**VA2**) functionalized microspheres following incubation with only the FITC-labeled noncomplementary target (blue); incubated simultaneously with equivalent concentrations of the noncomplementary DNA target and VEGF (red), incubated first with VEGF and then with the noncomplementary target (green); and incubated first with noncomplementary DNA target and then with VEGF (purple) under two annealing conditions: no anneal (**NA**), annealed prior (**PA**) to incubation with the noncomplementary DNA target.

Figure 4.2.3 shows the qualitative results for hybridization of the **AA**-functionalized particles when serially incubated with VEGF as a companion data set to the previous two figures. This study was included as a negative control to determine if VEGF presence would affect the hybridization efficiency of a particle functionalized with an aptamer that does not bind VEGF. It was observed that VEGF presence before or after incubation with the complementary target did not significantly affect duplex formation between the ampicillin aptamer and its primary DNA target.

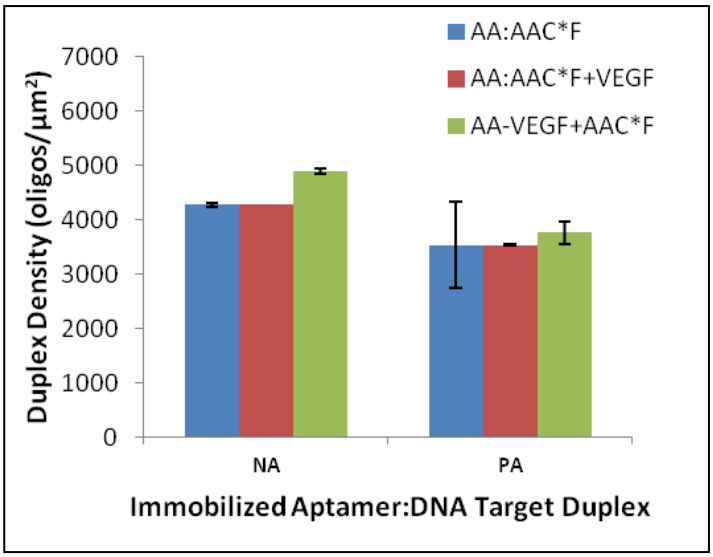


**Figure 4.2.3:** Surface densities of the aptamer:DNA target duplexes of ampicillin aptamer (**AA**) functionalized microspheres following incubation with FAM-labeled complementary DNA target only (**AA:AAC*F**); incubated first with the complementary target, and then with VEGF (**AA:AAC*F+VEGF**); and incubated first with VEGF and then the labeled complementary DNA target (**AA+VEGF, +AAC*F**) under two annealing conditions: no anneal (NA) and annealed prior (PA) to incubation with the complementary DNA target.

Figure 4.2.4 shows the qualitative results from a companion study to the one shown in Figure 4.2.1 using the unlabeled DNA target to evaluate the effects of the co-presence of both primary targets on binding. For this study, VEGF was labeled as previously described using the Luminex labeling kit with the PE-streptavidin molecules to directly measure relative VEGF binding to the aptamer-functionalized particles. Additionally, for this study only **VA1**-functionalized particles are analyzed since the success of displacing VEGF with DNA for the **VA2**-functionalized particles appears less likely as discussed earlier.

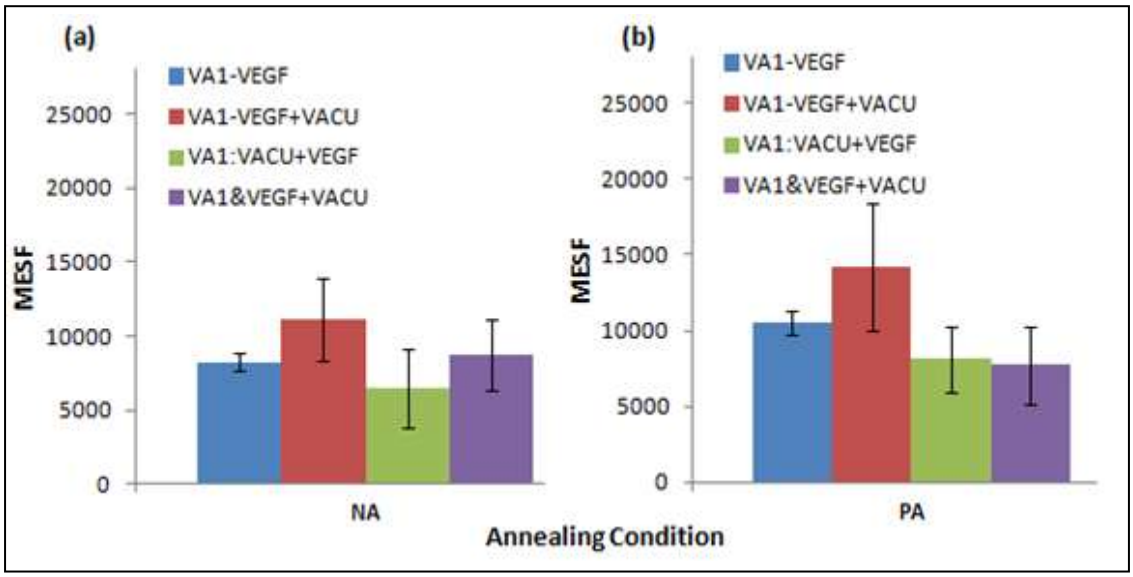


**Figure 4.2.4:** Molecules of Equivalent Soluble Fluorophore (MESF) measured from adding phycoerythrin (PE) to VEGF incubated with VEGF aptamer 1 (**VA1**) functionalized microspheres, showing incubation with only the PE-labeled VEGF, aptamer functionalized microspheres incubated with the unlabeled DNA target first and VEGF second, incubated with VEGF first and the unlabeled DNA target second, and simultaneously incubated with equivalent concentrations of the unlabeled DNA target and VEGF when no anneal (**NA**) was applied to the microspheres (a) or annealed prior (**PA**) to the first incubation (b).

The inclusion of the complementary primary DNA target was shown to have little effect on VEGF binding to **VA1**-functionalized particles when no anneal has been performed on the suspensions. Based on previous studies, this could indicate that **VA1** is capable of binding both of its primary targets simultaneously because neither target suffers a decrease in binding activity to the aptamer-functionalized particles when its counterpart is present. Thus, this choice in complementary DNA target maynot have a sufficient affinity advantage to serve as a displacement agent for VEGF bound to particle-immobilized aptamers. It may be possible that the inclusion of a synthetic oligonucleotide residue such as a locked nucleic acid (LNA) may be necessary to drive the release of the protein target from these immobilized aptamers. As shown previously by the Milam lab,[1] LNA mixmers, sequences containing DNA and LNA residues,

possesses a higher affinity for the **A20** probe strand, forming more duplexes than its pure DNA counterparts. Moreover, LNA mixmers also served as effective displacement agents for pure DNA or for shorter or mismatched LNA targets. Thus, future experiments could explore LNA as a displacement agent for VEGF bound to aptamers for potential recovery of the aptamer's dual binding activity.

## 4.3 Conclusions

Coincubation and serial incubation of the primary DNA and protein targets with aptamer-functionalized microspheres was investigated to elucidate the dual binding nature of the VEGF aptamer sequences. **VA1** and **VA2** showed distinct responses to these studies. **VA1** seemed to nonpreferentially bind to either of its primary targets, potentially indicating that it is capable of binding VEGF, perhaps even to an aptamer hybridized to its DNA target. Single-stranded **VA2**, however, seemed to favor binding VEGF over its primary DNA target. Serial incubation of the DNA target followed by VEGF and coincubation of both targets, showed that **VA2** bound less of its DNA target when VEGF was present and may indicate that it undergoes a conformational change to bind it protein target, blocking off the hybridization region of the aptamer sequence to our currently chosen DNA target.

## 4.4 References


1. Eze, N.A. and V.T. Milam, *Exploring locked nucleic acids as a bio-inspired materials assembly and disassembly tool.* Soft Matter, 2013. **9**(8): p. 2403-2411.
2. Battig, M.R., B. Soontornworajit, and Y. Wang, *Programmable Release of Multiple Protein Drugs from Aptamer-Functionalized Hydrogels via Nucleic Acid Hybridization.* J. Am. Chem. Soc., 2012. **134**(30): p. 12410-12413.

# CHAPTER 5

# REGENERATION OF APTAMER FUNCTIONALIZED COLLOIDAL PARTICLES THROUGH DNA MEDIATED INTERACTIONS

## INTRODUCTION

This chapter details using secondary hybridization events to trigger the release of DNA targets from aptamer:DNA target duplexes with the goal of fully recovering the binding activity of aptamers for either VEGF or DNA targets. Samples were prepared without any annealing step, as the objective was to achieve full recovery of the aptamer's functionality without requiring the colloidal system to be exposed to further heat treatment, so that these interactions might be implemented *in vivo* in the future and to minimize the time required to reset the system for reuse *in vitro*. For this purpose two separate studies were performed. The first to evaluate secondary hybridization as a viable method to initiate the full release of aptamer:DNA target duplexes using a displacement agent (**DA**) and then achieve comparable levels of primary hybridization, following displacement of the original DNA target, while a final study evaluated the effects of DNA release on VEGF binding to the now unoccupied immobilized aptamers. An overview of the incubation series in shown in Figure 5.1.1, but the individual steps are highlighted in subsections.

## 5.1 Experimental Setup

### 5.1.1 Displacement of Primary DNA Target via Hybridization of Primary DNA Target to the Displacement Agent

Primary hybridization was performed on two sets of samples as previously described[1], using 100 µL of 2 µM labeled (**VA1C*F**) or unlabeled (**VA1C**) complementary DNA. The incubation period of 8 hrs was chosen for these experiments. Following primary hybridization, three washed were performed at 9900g for 5 min, and the samples were resuspended in 500 µL of PBS/T, as previously described[2]. The samples were split into 100 µL aliquots. One of these aliquots was saved as a positive control to verify primary hybridization for the labeled complementary target. Four 100 µL aliquots were then taken and incubated with the secondary unlabeled hybridization partner (**DA**) or a noncomplementary unlabeled sequence. Two samples were prepared for complementary secondary hybridization and one for the noncomplementary case.

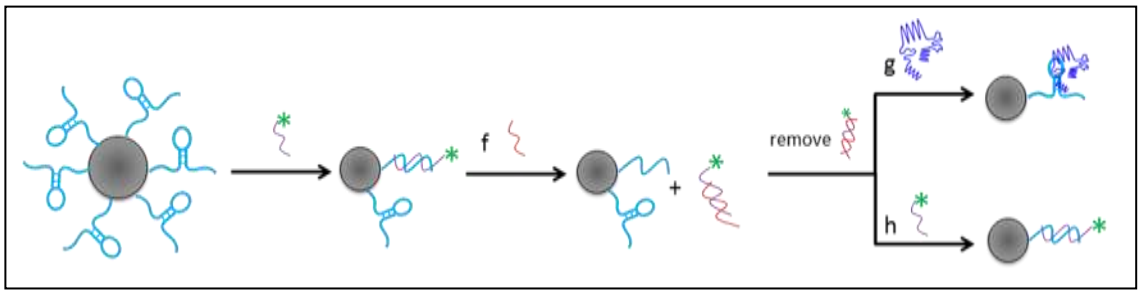


**Figure 5.1.1:** An Illustration showing how Aptamer:DNA target duplexes are incubated with (f) DNA displacement agent followed by removal of soluble duplexes followed by incubation with either (g) DNA target or (h) VEGF. In each case only one target species is labeled. Labeled DNA is conjugated with a FITC tag (*) on its 5' end. VEGF is labeled with phycoerythrin as illustrated in Scheme 3.

### 5.1.2 Subsequent incubation of recycled aptamers to either VEGF or DNA target

The secondary target is designed to hybridize to the primary target, using a four base long toehold on the 5' end of the DNA. Successful secondary hybridization induces

the release of hybridized DNA and possibly a return to the original, unannealed state of the aptamer. One of the two aliquots from the complementary secondary hybridization were then washed and incubated with either the labeled primary DNA target or VEGF, in the case of the **VA1C** primary hybridization, as previously described. VEGF was labeled using the streptavidin associated PE label from the Luminex kit as previously described, and all samples were prepared for analysis using flow cytometry as previously described by the Milam lab.[2] The particle suspensions were diluted to 1 mL using PBS/T following three washes (centrifugation at 9900xg for 3 min and resuspended in 100µL PBS/T) . The 1 mL suspensions were analyzed on a Becton Dickinson LSR II flow cytometer (Becton Dickinson, San Jose, CA) using FACSDiva software (Beckton Dickinson). Calibration curves was generated using Quantum FITC-5 MESF standards (Bangs Laboratories, Fishers, IN) or Quantum R-PE MESF standard (Bangs Laboratories, Fishers, IN) and were diluted in the same buffer as the samples, allowing quantification of fluorescence intensity in molecules of equivalent soluble fluorophore (MESF). MESF units from the standards are used to convert the mean fluorescence of each sample to the mean number of targets associated to each particle. Suspensions of EDAC activated 1 µm PS beads, unactivated 1 µm PS beads, and DNA functionalized beads mixed with a noncomplementary target were included to verify that all hybridization corresponds to specific interactions between complementary DNA sequences.

## 5.2 Results and Discussion

### 5.2.1 Regeneration of Hybridization Activity using Secondary Hybridization

Ultimately, we hope to design a system capable of repeated binding and release events for targeted therapeutic delivery, using aptamers. Therefore, it is necessary to evaluate the ability of the aptamer to both of it primary targets repeated after release and

recovery of the aptamer. To accomplish this, we examined particles functionalized with **VA1:VA1C*F** duplexes and attempted to displace the DNA target from the duplex using a DNA displacement agent (**DA**). The **DA** sequence was designed to be fully complementary to the primary DNA targets, to allow all 20 bases present in the primary target hybridize to the displacement sequence and overcome the shorter in comparison to the 16 base-long hybridization segment between the target and its aptamer's sequence. The toehold region mentioned previously and shown underlined in Table 2.1.1 is a short segment of nucleotide, that a freely presented to the surrounding suspension and serve as a nucleation point for hybridization between the displacement agent and the primary DNA target, to promote displacement of the primary target. As described above, **VA1**-functionalized particles were incubated with their FAM-labeled DNA target and allowed to hybridize. As a control, the hybridized aptamer-functionalized particles were incubated with a noncomplementary sequence to confirm that any DNA target release must be due to displacement by **DA**, and not due to simple duplex dissociation. Finally, the FAM-labeled DNA target was reintroduced to evaluate the ability of the **VA1** aptamer to rebind its DNA target. As shown in Figure 5.2.1, incubation with the noncomplementary sequence does not affect the observed duplex densities; however, loss of the fluorescence associated with the DNA duplexes was introduced indicating that the reduction in duplex density must be due to successful displacement of the DNA target. The second incubation with the DNA target resulted in comparable duplex densities as aptamer-functionalized particles that had never been previously hybridized. Thus it was concluded that full recovery of aptamer binding activity to DNA target was achieved.

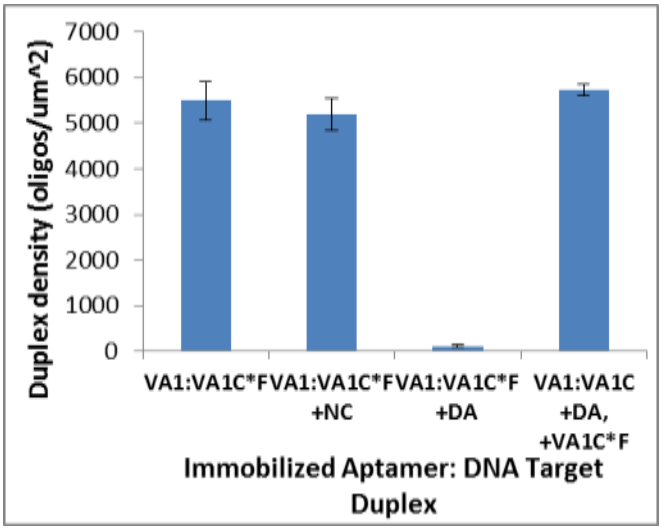


**5.2.1** Surface densities of aptamer:DNA target duplexes incubated under the following conditions: with the labeled DNA target (**VA1C*F**) alone, with the labeled DNA target followed by an unlabeled noncomplementary target (**NC14**), with the unlabeled complementary DNA target (**VA1C**) followed by the displacement agent (**DA**), and finally with the unlabeled complementary DNA target followed by the displacement agent and then incubated with the labeled complementary DNA target.

After verifying that recovery of the aptamer's hybridization efficiency was possible, it was necessary to evaluate that aptamer's ability to bind VEGF following displacement of the primary DNA target from the duplexes. Therefore, samples were prepared by hybridizing **VA1**-functionalized particles, displacing the primary target, and then incubating the now unoccupied aptamers with VEGF. Figure 5.2.2 shows these results as well as data for VEGF binding to particles that have not been annealed at any point during preparation. This data set was chosen for comparison because ideally the system would be capable of cyclic binding and release without further processing. Also included is a control in which VEGF was not incubated after the displacement agent to show that the displacement of the DNA target does not provide another source of nonspecific interactions for the PE labeling components. Figure 5.2.2 shows VEGF binding is greater to single-stranded aptamers prior to displacement events. Thus,

previously occupied **VA1** aptamers were not able to fully recover binding activity to VEGF.

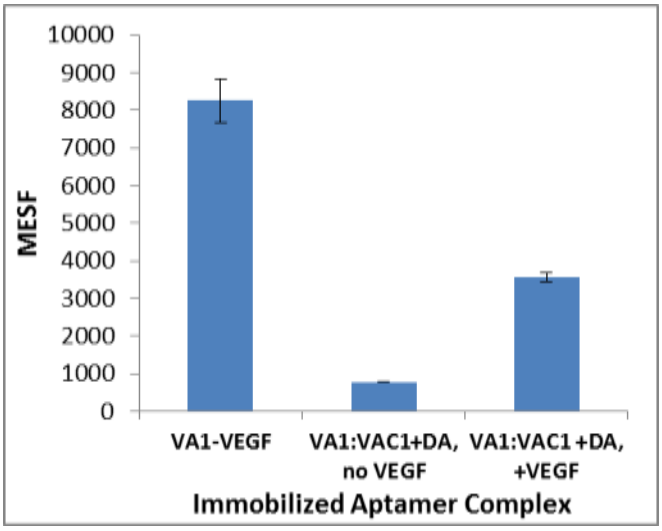


**Figure 5.2.2:** Molecules of equivalent soluble fluorophore (MESF) measured from adding phycoerythrin (PE) to **VA1**-functionalized microspheres following incubation with VEGF only (**VA1-VEGF**); following incubation with the unlabeled complementary DNA target, then displacement agent (**VA1:VA1C+DA, no VEGF**) and finally incubated with VEGF (**VA1:VA1C+DA, + VEGF**).

## 5.3 Conclusion

Recovery of the aptamer's dual binding nature was evaluated following displacement of the primary DNA target using a displacement agent designed to possess a higher affinity for the primary DNA target than the aptamer. Full recovery of the aptamer's ability to bind its DNA target after recovery of the unbound immobilized aptamer was achieved; however, only partial recovery of the aptamer's ability to bind VEGF was observed. Full recovery may be possible following the inclusion of a new annealing treatment, but our desire is to develop a system capable of repeated binding and release events in vivo; therefore, the effects of a separate anneal have not been tested at this time.

## 5.4 Future Outlook

In the future, it would be interesting to repeat this process for **VA2**; since it has shown signs of VEGF binding using the induced fit model; it may be capable of more complete recovery of its binding activity to VEGF. Additionally as previously discussed the inclusion of LNA residues in the DNA sequences, both aptamer and target, is of interest. LNA offers greater nuclease resistance and higher affinity for immobilized DNA probes,[2] but complications arising from the more rigid structure, due to the restricted conformation of the sugar in the LNA backbone, would need to be assessed. Development of a PE label of known size (i.e. fluorescent polymeric subunits) and an appropriate standard should be a priority for future studies to directly monitor the binding activity of VEGF molecules to immobilized aptamer sequences. Finally, using a similar method as those outlined in this work to immobilize the blocking agent sequence, it would be possible to begin the development of a dual aptamer system for the delivery of multiple therapeutic molecules.

## 5.5 References


1. Tison, C.K. and V.T. Milam, *Reversing DNA-Mediated adhesion at a fixed temperature.* Langmuir, 2007. **23**(19): p. 9728-9736.
2. Eze, N.A. and V.T. Milam, *Exploring locked nucleic acids as a bio-inspired materials assembly and disassembly tool.* Soft Matter, 2013. **9**(8): p. 2403-2411.

# APPENDIX A

## Calculation of the DNA Concentration via UV-vis Spectral Analysis

As previously described, the DNA sequences were aliquoted and stored using Tris-EDTA (TE) buffer. FAM-labeled DNA sequences were stored in 10 µL aliquots at 100 µM in pH 8.0 TE, and the unlabeled targets and aminated sequences were stored at the same concentrations in 20 µL aliquots using pH 7.4 TE buffer. Prior to incubation or coupling the samples were diluted to the appropriate concentrations as described in the previous chapter, depending on the experiment. To verify the concentration of the DNA solutions, UV-vis analysis and the Beer-Lambert law, shown below, were applied. IDT reports the individual extinction for all DNA sequences they synthesize.

$$A=\varepsilon lc \tag{1}$$

A corresponds to the measured absorbance of the DNA solution using UV-vis. The variables ε, *l*, and *c* correspond to the extinction coefficient, path length (the distance light travels through the material), and the concentration respectively. For our purposes the path length is equal to 1 cm. Samples of 150 µL (2 µM), diluted from 10 µL aliquots (100 µM), were analyzed and curves of wavelength (nm) vs. absorbance were generated. The characteristic peak associated with DNA occurs at 260 nm, and the measured value of absorbance at this concentration is used for concentration calculations. Figure A1 below shows a representative curve for the DNA solutions.

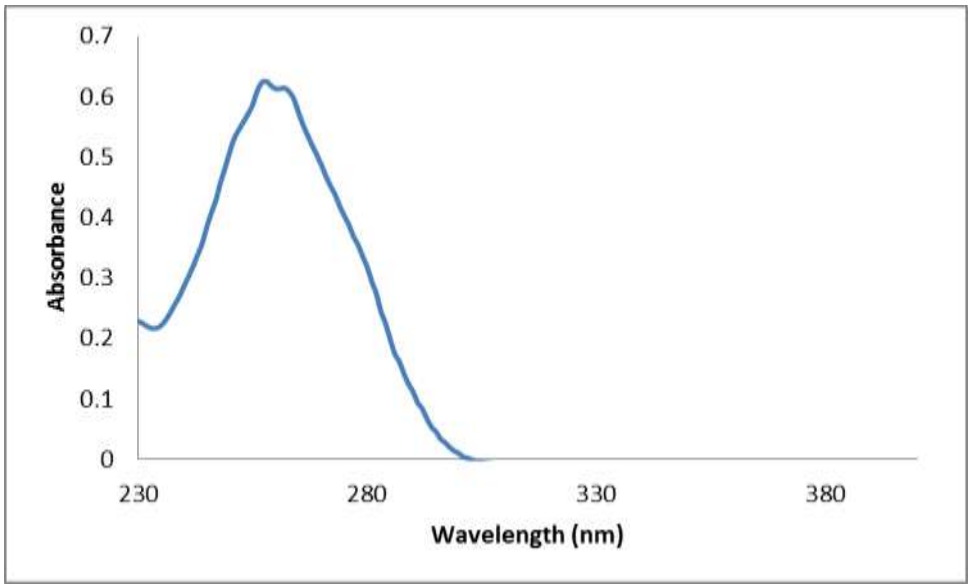


**Figure A.1:** Plot of wavelength vs absorbance generated via UV-vis analysis of VEGF Aptamer 1 (**VA1**) DNA in solution, showing the characteristic peak at 260.

Additionally, a NanoVue Plus Spectrophotometer (GE Healthcare, Picataway, NJ) was used to verify the concentrations measured with the UV-vis spectrometer. All concentrations calculated with the two spectrometers agreed. Table A1 lists the average calculated concentrations for each of the relevant sequences.

**Table A1:** Calculated concentration of soluble DNA, using spectral analysis techniques.

| Sequence | Concentration (μM) |
|---|---|
| **VA1** | 2.30 |
| **VA2** | 2.20 |
| **AA** | 2.05 |
| **A20** | 1.70 |
| **VA1C*F** | 2.30 |
| **VA1C** | 2.15 |
| **VA2C*F** | 2.45 |
| **AAC*F** | 2.20 |
| **B15*F** | 2.40 |
| **DA** | 1.98 |
| **NC14*F** | 2.25 |
| **NC14** | 2.05 |
| **NC18*F** | 2.23 |

# APPENDIX B

## Calculation of the Radius of Gyration for PEG and VA1 Aptamer Sequence

Incorporation of 5 kDa PEG as a blocking agent lead to significant loss in hybridization of immobilized aptamer sequences, as shown in Chapter 2. To better understand the cause of this phenomenon the effective radius of gyration for both PEg and the **VA1** aptamer sequence were calculated using the following equations.

$$R_g^2 = \frac{l*L_p}{3} - L_p^2 + \frac{2L_p^3}{l} - \frac{2L_p^4}{l^2}\left(1 - e^{\frac{-l}{L_p}}\right) \quad (1)$$

$$<R^2> = C_\infty n l^2 \quad (2)$$

Equation 1 is used to calculate the length of the extended aptamer sequence. $L_p$ is the persistence length. For ssDNA $L_p$ is equal to 4.6 nm. The variable l is a function of N, the number of bases in the sequence, and a, the effective nucleobase length (0.6 nm for ssDNA). Using these values the radius of gyration for the immobilized aptamer was calculated to be 9.22 nm in length.

Equation 2 is uses the ideal chain model to calculate the length of the PEG polymer chain. $C_\infty$ is the Flory-Huggins characteristic ratio and is equal to 6.7 for PEG. The variables *n* and *l* correspond to the number of repeat units in the polymer chain and the length of the repeat unit respectively. For PEG *l* is equal to 1.1 nm. The PEG molecule utilized in this study was 5 kDA in size, corresponding to a chain of 173 repeat units. $R_g$ was calculated to be 30.27 nm for 5 kDA PEG, meaning the elongated PEG strand was approximately three times the length of the aptamer sequence.